CLEAVAGE OF AROMATIC CARBON-CARBON BONDS

Eugene A. Kline and William P. Teichert

Department of Chemistry
Tennessee Technological University
Cookeville, Tennessee 38505

and

Bruce W. Farnum

University of North Dakota Energy Research Center
Box 8213, University Station
Grand Forks, North Dakota 58202

Introduction

The search for a model substrate to use in evaluating relative reactivity of H-donors, under coal liquefaction conditions has led to this study of o-terphenyl.

The stability of biphenyl, terphenyls, quaterphenyls, and polyphenyls in the absence of H-donors has been demonstrated by their high bond dissociation energies between aromatic rings (1, 2). Therefore, they have practical application as coolant moderators in nuclear power plants (3). This stability is gained in part from the orbital overlap of the carbon atoms in the interannular C-C bond. The melting point of p-terphenyl is 208°C, and of hexiphenyl is 469°C. Their UV absorption at 278 and 318 nanometers, respectively, are indications of the increased stability as the number of benzene rings increases and resonance stabilization increases. The thermal temperature (defined as the temperature ±10°C at which decomposition rate is 1 mole % per hour) for m-terphenyl was 485°C and for the p-isomer was 478° (3). The same workers studying the problem of polymerization of polyphenyls and its control in nuclear power plants found one solution to the build up of the high molecular weight polymers. Reclamation by catalytic hydrocracking to reduce molecular weight in every case lowered the decomposition temperature to 320°-400°C due to formation of 20% methylated and ethylated products.

Reaction of polyphenyls under coal liquefaction conditions has been reported (4). The compound o-terphenyl (OTP) was found to couple irreversibly to form the very thermally stable triphenylene in the presence of an H-donor without a catalyst. Formation of different amounts of triphenylene with different H-donors suggested that o-terphenyl was a good candidate as a model substrate for study of the relative abilities of H-donors to react. Two other model substrates, 1,1'-binaphthyl (5) and dibenzo(c,g)phenanthrene (4), were also found to couple at different rates indicating they, too, would be possible substrates which could be used to differentiate the effectiveness of H-donors. Dibenzo(c,g)phenanthrene was difficult to prepare, and it coupled in the absence of H-donor and gave other hydrogenated isomers without coupling. o-Terphenyl formed extremely small amounts of coupled product compared to 1,1'-binaphthyl; consequently, the latter was judged to be the best model substrate of the three compounds to use in studying the effect of H-donors on the coupling reaction.

An unexpected result in the reaction of o-terphenyl and H-donors without catalyst was the large production of biphenyl. As much as 60%

cleavage reaction to yield biphenyl was observed while coupling reaction to yield triphenylene was always less than 5%. The rates of biphenyl formation varied with the particular H-donor used, suggesting that this cleavage reaction can be used to compare reactivity of H-donors at high temperatures. This paper discusses results of cleavage reaction studies with o-terphenyl.

Results and Discussion

All reactions were carried out in 1/2" Gyrolok, Parker, or Swagelok unions. Equimolar amounts of H-donor and o-terphenyl were added to the reaction vessel. It was filled with benzene solvent, and sealed without addition of a gas. The reactor was then placed in a fluidized sand bath controlled at 470±2°C. Analyses of the resulting product mixtures were carried out on a gas chromatograph programmed 75°-300° at 15°/min, 6' x 2 mm ID Dexsil 300 column.

The determination of kinetic rate constants provided some insight into the mechanism of the reaction. Reactions were run for 1, 2, 3, 4, and 5 hours with equimolar amounts of several model H-donors that were able to withstand the severe conditions. Mass balance was obtained in most cases accounting for both H-donor and o-terphenyl. The appearance of triphenylene and biphenyl were fitted to both first order and autocatalytic rate expressions. The best fit for the appearance of triphenylene was the autocatalytic rate expression; however, the first order expression correlated nearly as well. The formation of biphenyl appeared to fit the pseudo first order rate expression. The resulting yields and rate constants for the various H-donors with o-terphenyl to form triphenylene and biphenyl are shown in Table I.

The rate constants for the formation of triphenylene with different H-donors over five hours compared relatively well with the one-hour yield data. Hydrogenated heterocycles such as tetrahydroquinoline were too thermally-unstable to study under these conditions. The fact that triphenylene and biphenyl formation fit different rate expressions was significant. The autocatalytic formation of the coupled product (triphenylene from OTP) suggested that another species (perhaps the hydrogenated intermediate) was involved in the coupling. As this species was generated more coupling occurred.

A radical capping mechanism did not explain the kinetics data. Rather, coupling of the o-terphenyl by induction by a secondary H-donor seemed more justifiable. The 9,10-dihydrophenanthrene decomposed to a very small concentration within one hour (4), yet triphenylene continued to increase. Even in the case of tetralin which decomposed at a constant rate, there appeared to be autocatalytic formation of the coupled product.

Another way to investigate the mechanism was to study the differences and similarities of reactions of the isomeric terphenyls. Since cleavage was involved, the ortho-isomer had no predictable advantage as a model substrate. Two of the isomers, m-terphenyl and o-terphenyl were reacted with one H-donor, tetralin, for 1, 2, 3, 4, and 5 hours, and the products were analyzed by the usual method. p-Terphenyl was found to be quite insoluble in most solvents and reaction times of 1, 3, and 5 hours were selected. The results are summarized in Table II.

One deuterated H-donor 9,9,10,10-d_4-9,10-dihydrophenanthrene was reacted for three hours with o-terphenyl in benzene. The tendency toward random scrambling from the deuterated H-donor to the produced

biphenyl was studied by reacting the deuterated H-donor with biphenyl under the same conditions in a separate experiment. Due to excessive exchange, no clear cut mechanistic information was obtained.

The application of this reaction of o-terphenyl to determine relative reactivity of coal-derived liquids was studied by reacting equal weights of o-terphenyl and various start up and coal-derived recycle solvents produced in the UND Energy Research Center continuous process coal liquefaction pilot plant. The liquids used were from the ends of runs which had undergone several recycle passes in a reducing atmosphere, and which have been well characterized (6). The results of the reactions are summarized in Table III. The values of biphenyl produced were obtained by the difference of the biphenyl after reaction and the initial amount of biphenyl in the coal liquid.

The unique feature in the three hour o-terphenyl reactions was the formation of biphenyl in significant quantities in most cases and in differing amounts showing differences in the ability of the solvents to affect this cleavage. One thing noticeably different in running these reactions was the small amount of gas pressure in the reactor at the end of the reaction compared with the hydrogenated model H-donors.

In summary, o-terphenyl couples in the presence of model H-donors and many coal derived solvents to form triphenylene, and forms biphenyl by cleavage. The latter reaction is of more interest as the yields are substantial, and the yields have application to the study of properties of solvents. Attempts to elucidate the mechanism involved kinetic studies, and reaction with a deuterated H-donor. The best mechanism appears to be that in which the low steady-state concentration of reactive H-donor attacks either ipso position in o-terphenyl followed by cleavage (7). This mechanism is known to occur at high temperatures.

Literature Cited

1. Streitweiser, Jr., Andrew; and Heathcock, Clayton H. "Introduction to Organic Chemistry," 2nd ed., McMillan Publishing Co., Inc., 1194 (1981).
2. Vernon, Lonnie W. Fuel, 59, 102 (1980).
3. Scola, Daniel A.; and Adams, Jr., John S. Ind. Eng. Chem. Prod. Res. Develop., 10, 417 (1971).
4. Kline, Eugene A.; and Farnum, Bruce W. Am. Chem. Soc. Div. Fuel Chem. Preprints, 28, 155 (1983).
5. Kline, Eugene A.; Harrison, Mark E.; and Farnum, Bruce W. Am. Chem. Soc. Div. Fuel Chem. Preprints, 27, 18 (1982).

6a. Farnum, Sylvia A.; Farnum, Bruce W.; Bitzan, Edward F.; Willson, Warrack G. and Baker, Gene G. Fuel 62, 799(1983).

b. Quarterly Technical Progress Report DOE/FC/QTR 82/2 (DE83013383) Grand Forks Energy Technology Center, Grand Forks, ND (1983).

c. Runs 101 and 103, Unpublished Results, UNDERC.

7. McMillan, Donald F.; Ogier, Walter; Chang, Sou-jen; Fleming, Ronald H.; and Malhotra, Ritudamin. Proceedings of International Conference on Coal Science, Pittsburgh, PA, August 15-19, 1983, pp. 199-203.

Table I. Results of Reactions of H-Donors and o-Terphenyl

H-Donor	Triphenylene* Yield	k(/sec) ($\times 10^3$)	Biphenyl** Yield	k(/sec) ($\times 10^3$)
Blank	0.1	--	3%	--
1,2,3,4-detrahydro-naphthalene	2.9%	7.2	60	1.9
1,2-Dihydronaph-thalene	2.7	--	54	1.3
1,4-Dihydronaph-thalene	2.5	6.4	4	1.3
Fluorene	2.9	1.6	60	1.4
Indane	7.1	9.8	30	2.5
Indene	3.7	8.5	46	1.8
9,10-Dihydrophen-anthrene	3.2	7.0	34	2.6
9,10-Dihydroan-thracene	1.0	3.3	47	1.6

*Triphenylene/initial OTP (one hour reaction) (autocatalytic)
**Biphenyl/initial OTP (five hours reaction) (Pseudo first order)

Table II. Results of Reactions of the Terphenyls with Tetralin at 470°C (rate constants - x 10^3 min^{-1})

o-Terphenyl	m-Terphenyl*	p-Terphenyl*
k=2.0	k=2.4	k=2.0

*Modelled pseudo-first order as best fit.

Table III. Results of Reactions of Coal Derived Liquids with o-Terphenyl at 470°C for 3 Hours

Coal Derived Solvent	Origin of Solvent	Biphenyl (RXN)-Biphenyl (INIT)
101PB21	Zap, ND lignite, pass 12[a]	68%
101PB40	Zap, ND lignite, pass 40[a]	37
67PB23	Wyodak Subbituminous, pass 12[a]	5
64PB25	Big Brown-Texas lignite,[a] pass 13	67
65PB23	Beulah, ND lignite, 12 passes[a]	67
53PB18	Powhatan Bituminous, pass 18[a]	38
Project Lignite Recycle Solvent	Zap, ND lignite, UND PDU	28
Crowley A04	Typical Anthracene Oil	13
SCR Mid. Dist.	Fort Lewis Pilot Plant (Powhatan coal)	25

a)Recycle solvents from the University of North Dakota Energy Research Center continuous process unit.

ARYLATIONS OF COAL MODEL SYSTEMS

Barbara F. Smith, Clifford G. Venier, and Thomas G. Squires

Applied Organic Chemistry,
Energy and Mineral Resources Research Institute,
Iowa State University, Ames, Iowa 50011

Currently, coal is converted to clean liquids or low melting solids by processes which utilize high temperature, high pressure, or both. These processes occur by thermal bond cleavages and involve the intermediacy of free radicals. In a search for chemistry which could liquefy coal under milder conditions, we have focussed on thermally less demanding ionic reactions.

Of the functional groups which commonly occur in coals, ethers are the easiest to cleave under acid conditions. Depending on the density of these linkages and their importance as crosslinks in the macromolecular structure of coals, solubilization might be greatly enhanced solely by cleaving and capping ether bonds. Benzylic ethers are particularly reactive and have been implicated in the initiation of coal pyrolysis(1) and hydropyrolysis(2). Arylation, the use of acids to cleave bonds in coals in the presence of aromatic rings to trap the consequent incipient carbonium ions, has a long history(3). The most extensively studied system is the Heredy-Neuworth phenol depolymerization(4).

We have chosen to use benzyl phenyl ether and 1-naphthylmethyl phenyl ether and polymers related to them as models to develop and evaluate the chemistry involved in the arylations.

RESULTS

Arylmethyl phenyl ethers undergo competing reactions when treated with Lewis acids. A partitioning of arylmethyl groups between an intramolecular process (a rearrangement) and an intermolecular one can be seen in Table 1. The fact that the rearranged product is overwhelmingly the ortho isomer is consistent with the intramolecular

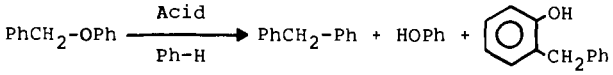

(1)

nature of the rearrangement(5). Regardless of the choice of acid or temperature, essentially one-half of the starting phenylmethyl phenyl ether, **1**, ends up as rearranged product. Table 2 shows that generally the same result holds for 1-naphthylmethyl phenyl ether, **4**. However, a previously unrecognized complication shows up in the products of the acid-catalyzed reaction of **4**.

Despite the fact that solvent benzene is in great excess, substrate or product or both, effectively compete for the 1-naphthylmethyl moiety. Capillary gc-ms reveals that at least five products of molecular weight 374 are produced in these reactions. This corresponds to structures containing two 1-naphthylmethyl groups and one phenol. These products can arise by substrate capture of a 1-naphthyl-methyl followed by ether-to-phenol rearrangement or, alternatively, by capture of 1-naphthylmethyl by products **5**. Even under conditions where the molar ratio of benzene to starting material

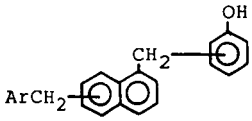

21 isomers possible

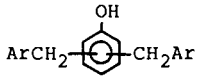

6 isomers possible

exceeds 1000, a significant number of product molecules derive from more than one molecule of starting ether.

If substrate and/or products can trap the electrophilic 1-naphthylmethyl species with such efficiency, it stands to reason that other aromatic compounds will likely be better than benzene also. Table 3 shows data demonstrating that this is the case. The fact that the relative rate constant measured for the naphthalene-benzene competition remains constant over a 100-fold change in naphthalene concentration, confirms that the change in product slate arises by the simple partitioning of an intermediate between the two traps. The straightforward behavior of the system was further checked by allowing diphenylether and 2,6-dimethylphenol to compete directly. The rate constants determined when three traps are present are sensibly the same as those found in binary competition (see last line of Table 3).

One would expect the same sort of behavior for the trapping of intermediates generated from insoluble materials. Naphthalene should be a substantially better capping agent than benzene. The results of the BF_3-catalyzed arylations of polymer **9** with benzene, naphthalene, or phenanthrene as traps in CH_2Cl_2 solvent are given in Table 4, along with the results from some reactions carried out in benzene solvent.

Of particular importance is the fact that the solubilities of products generated in the presence of naphthalene and phenanthrene differ markedly from that produced by BF_3 treatment alone. Infrared spectra clearly establish that the ether functions present in the starting polymer are no longer present in the products. Apparently, in the absence of a trap, polymer **9** is converted to a new polymer, whose structure is best approximated as **10**, equation 2, although we recognize that substantial amounts of interchain crosslinking might occur. The enhanced solubility in the presence of arene, therefore, signals the lowering of molecular weight by capping reactions, equation 3.

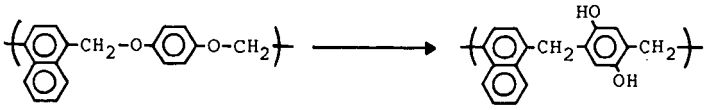

(2)

9 10

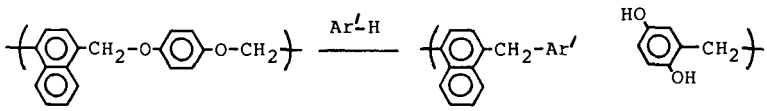

(3)

DISCUSSION

The results reported here are best interpreted on the basis of a model in which carbonium ions generated from arylmethyl phenyl ethers are partitioned between the various nucleophiles present. In this system, aromatic rings are the most nucleophilic functional groups. The 1-naphthylmethyl cation is much more stable than is the simpler

$$PhO\text{-}CH_2Ar \xrightarrow{BF_3} PhOBF_3^- + ArCH_2^+ \xrightarrow{Ar_iH} ArCH_2Ar \qquad (4)$$

benzyl cation, and, consequently, much more selective in its reactivity(6). Thus, in the case of benzyl phenyl ether, **1**, solvent benzene effectively traps all generated carbonium ions. However, the more stable 1-naphthylmethyl cation generated from **4**, is sufficiently stable to discriminate between the poorly nucleophilic benzene and the more nucleophilic molecules, **4** and **5**. Naphthalene, on the other hand, is much more nucleophilic than benzene(7), and in sufficient concentration, suppresses "self-trapping".

The same picture emerges from work with polymer **9**. Apparently, benzene is insufficiently reactive to compete with intramolecular (intrapolymer) nucleophiles and, consequently, no increase in solubility accompanies the cleavages of ether links in **9** upon addition of benzene. When better nucleophiles, naphthalene and phenanthene, are provided, carbonium ions generated from ether cleavages <u>are</u> capped and the product is lower in molecular weight and more soluble.

It is worth noting that the naphthalene (k_{rel}=280) is nearly as good a trap as the phenol (k_{rel}=450). Since hydroxylic solvents will level the acid strength of BF_3 to that of $ROBF_3^-H^+$ and hydrocarbons would not, the acid-catalyzed bond cleavages necessary for unlinking coal may in fact be faster in BF_3-arene than in BF_3-phenol. While we have not yet extended these results to coals, we believe that the combination of a relatively mild Lewis acid catalyst, BF_3, with a good carbonium ion trap, naphthalene, will allow selective cleavage and capping of aryl alkyl ether bonds.

EXPERIMENTAL

All gas chromatographic (GC) analyses were performed on a Tracor model 550 gas chromatograph with flame ionization dectector; glass columns were 6'x4mm and 6'x2mm, packed with 3% OV-1 or OV-101 on 80-100 mesh supelcoport, respectively. Columns were held at 80°C for 2 min. and then the temperature raised to 275°C at 25°/min and held for 10 min (benzyl phenyl ether reactions) or initially held at 120° and the temperature raised to 200° at 5°/min and held for 10 min (1-naphthylmethyl phenyl ether reactions). Peak areas were integrated by the "cut and weigh" method. NMR spectra were obtained on a Varian EM 360, IR spectra on a Beckman IR-4230 and GC-Mass Spectra on a Finnigan

4023. Liquid chromatographic analyses were carried out on a Varian 5000 LC with a Varian UV-50 detector at 270 nm.

Benzyl phenyl ether and 1-naphthylmethyl phenyl ether were prepared by reaction of phenoxide ion with the requisite halide, and purified by recrystallization. The polymer 9 has been previously described(8).

Reaction of Arylmethyl Phenyl Ethers with Lewis Acids in Benzene. General Procedure

The arylmethyl phenyl ether, internal standard (hexadecane or dodecane) and trapping agents (naphthalene, 2,6-dimethylphenol or diphenylether) when used, were placed in a dry flask and dissolved in benzene that had been dried by azeotropic distillation and stored over 4A molecular sieves. Lewis Acid (BF_3, BF_3-CH_3OH or $AlBr_3$) was then added as a dilute benzene solution or directly to the reaction mixture at room temperature. Aliquots were removed at timed intervals, quenched with water, and diluted for LC and/or GC analysis.

Reaction of Polymer 9 with Arenes Catalyzed by Lewis Acids

To a dry flask outfitted with a magnetic stirrer was placed polymer, 9, dry solvent (benzene or methylene chloride), and trap (naphthalene or phenanthrene) when used. Lewis acid was added, in most cases, as a dilute solution or, in a few runs with BF_3, as a gas. The heterogeneous mixture was stirred for the indicated time at the required temperature. The resulting blue-green reaction mixture was quenched with water, filtered and washed. The insoluble residue was dried, weighed and analyzed by IR. The organic filtrate was dried and the solvent removed under vacuum.

REFERENCES

1. Siskin, M.; Aczel, T. Fuel **1983**, 62, 1321.
2. Tanner, K.I.; Bell, A.T. Fuel **1981**, 60, 52.
3. Larsen, J.W.; Kuemmerle, E.W. Fuel **1976**, 55, 162.
4. Wender, I.; Heredy, L.A.; Neuworth, M.B.; Dryden, I.G.C. In "Chemistry of Coal Utilization. Second Supplementary Volume"; Elliott, M.A., Ed.; Wiley: New York, 1981; Chapter 8, pp. 447-454; and references therein.
5. Dewar, M.J.S. In "Molecular Rearrangements, Part 1"; de Mayo, P., Ed.; Wiley: New York, 1963; Chapter 5.
6. Streitwieser, A., Jr. Chem. Rev. **1956**, 56, 571.
7. Dewar, M.J.S.; Mole, T.; Warford, E.W.T. J. Chem. Soc. **1956**, 3581, report k(naphthalene)/k(benzene)=350 for nitration.
8. Squires, T.G.; Smith, B.F.; Winans, R.E.; Scott, R.G.; Hayatsu, R. Proc. Intern. Conf. Coal Sci. **1983**, 292.
9. Bunnett, J.F. In "Investigations of Rates and Mechanisms of Reactions"; Lewis, E.S., Ed.; Wiley-Interscience: New York, 1974; Chapter IV, pp. 158 ff.

Table 1. Products of Acid-catalyzed Phenylation of Phenyl Benzyl Ether.[a]

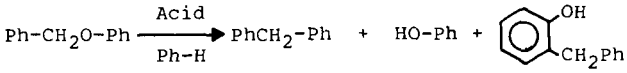

1	2	3
	intermolecular	intramolecular
ACID	**Ph_2CH_2**	**o-benzylphenol**
CF_3SO_3H	44%	48%
$BF_3 \cdot CH_3OH$	47%	40%
$BF_3 \cdot CH_3OH$ (72°)	49%	49%
BF_3	49%	48%
$AlBr_3$	48%	54%

[a]Room temperature, benzene solvent.

Table 2. Products of BF_3-Catalyzed Cleavage of 1-Naphthylmethyl Phenyl Ether.[a]

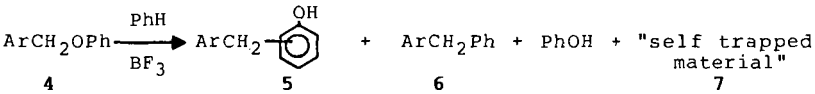

$ArCH_2OPh$	o-5	p-5	6	recovery	7[b]
0.2M	30	12	<1	43%	(1.00)
0.02M	37	15	6	58%	.76
0.002M	50	16	12	78%	.27

[a]Room temperature, benzene solvent

[b]Relative yield of several products from liquid chromatographic analysis.

Table 3. Relative Trapping Ability of Aromatic Compounds in BF_3-Catalyzed Cleavage of 1-Naphthylmethyl Phenyl Ether.[a]

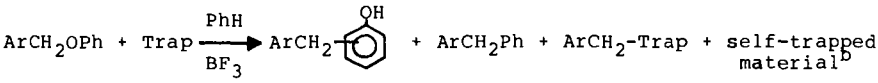

		5	6	8		7
Trap	Trap, M	o-5	p-5	6	8	k_{rel}[c]
Benzene	0	38	13	7	--	(1)
Naphthalene	.020	33	14	7	3	280
Naphthalene	.20	37	14	3	17	310
Naphthalene	2.0	32	8	1	46	260
Diphenyl Ether	.20	41	13	4	4	50
2,6-Dimethylphenol	.20	39	12	2	17	450
Diphenyl Ether	.20	28	9	1.5	15	500
2,6-Dimethylphenol	.20				1.3	45

[a]Room Temperature, benzene solvent.

[b]See Figure 1 for relative yields of self-trapped material.

[c] $\frac{k_{trap}}{k_{PhH}} = \frac{[ArCH_2\text{-}Trap]}{[ArCH_2Ph]} \times \frac{[PhH]}{[Trap]}$, see reference 9.

Table 4. BF_3-Catalyzed Arylation of Polymer 9.

			Product solubilities[a]		
ArH/solvent	Acid	Temp.	CH_2Cl_2	PhH	Acetone
CH_2Cl_2	$BF_3 \cdot H_2O$	23°			0%[b]
CH_2Cl_2	BF_3	20°	<5%		
PhH/CH_2Cl_2[c]	BF_3	20°	<5%		
naphthalene/CH_2Cl_2[c]	BF_3	20°	29%		
phenanthrene/CH_2Cl_2[c]	BF_3	20°	24%		
PhH	$BF_3 \cdot CH_3OH$	80°		11%	39%
PhH	BF_3	23°		19%	76%

[a]Determined by weight of insoluble product.

[b]IR shows complete loss of ether functionality.

[c]0.4 M Arene.

ACKNOWLEDGEMENT

This material was prepared with the support of the U. S. Department of Energy, Grant No. DE-FG22-82PC50786. However, any opinions, findings, conclusions, or recommendations expressed herein are those of the authors and do not necessarily reflect the views of DOE.

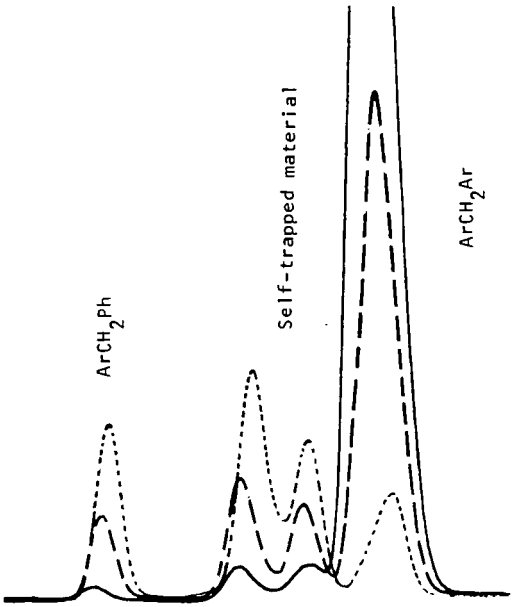

Figure 1. Liquid Chromatograms of the Naphthylation of 1-Naphthylmethyl Phenyl Ether, $ArCH_2OPh$ (see Table 3).

····· 0.020 M Naphthalene (ArH)

-------- 0.20 M Naphthalene (ArH)

———— 2.0 M Naphthalene (ArH)

BENZYLIC FUNCTIONALITY IN COAL DERIVED ASPHALTENES: A CALIFORNIUM-252 PLASMA DESORPTION MASS SPECTROMETRY APPROACH*

R.A. Zingaro, R.D. Macfarlane, J.M. Garcia III, A.G. Vindiola and J.H. Zoeller, Jr.
Department of Chemistry, Texas A&M University, College Station, Texas 77843

INTRODUCTION

The hydroaromatic components embodied in coal molecules strongly influence the thermal behavior of coal in a variety of conversion processes. A body of indirect evidence suggests that effects due to facile bond breaking at benzylic carbon atoms are operative in coal liquefaction (1,2), mesophase development (3,4) and devolatilization behavior (5). In an ongoing study of the structure of coal derived molecules by the technique of Californium-252 Plasma Desorption Mass Spectrometry (CFPDMS), we have found (6) that asphaltenes display positive ion groups of semiregular periodicity in the mass region 150 to 400 amu, and that this pattern is strikingly similar to that of pure hydroaromatic compounds. Such ion groups are also observed (7,8) in Field Ionization Mass Spectrometry (FIMS) spectra of coal derived materials. We wish to present evidence that such ion groups are due to benzylic functionalities and not to families of compound group classes.

The CFPDMS technique involves the use of the nuclide ^{252}Cf, one of whose modes of decay is spontaneous fission. Each fission event ejects two fragments in opposite directions, each with speeds of c/10, and energies of 80 to 150 MeV. Interaction of one of these fission fragments with a thin film of organic substrate generates a highly localized hot spot which devolatilizes positive and negative ions. In the CFPDMS experiment (9,10) these ions are accelerated towards a charged grid and into a time of flight (TOF) mass spectrometer. The TOF clock is triggered by the second, simultaneously ejected fission fragment colliding with a start detector and stopped when an organic ion collides with the TOF detector. Acquisition of the TOF data over many events is managed under computer control. Accumulated data is assembled into a mass spectrum by calibration with known common ions.

Native coal asphaltenes can be isolated from low rank coals by dimethylsulfoxide (DMSO) extraction and solvent fractionation. DMSO extraction of the Wilcox seam lignite lithotype yields almost a quarter of the organic matter present. From this extract is isolated the tetrahydrofuran (THF)-soluble, hexane-insoluble fraction, formally a asphaltene-preasphaltene blend. The positive ion CFPDMS spectrum of this sample displays the ion

* Dedicated to Professor Peter Given, honorable recipient of the 1984 Henry H. Storch Award in coal research.

groups described. Such ions are also seen in the spectra of asphaltenes and preasphaltenes from coal liquefaction products, and in the spectra of hydroaromatic compounds. The CFPDMS fragmentation pattern of 1,2,3,6,7,8 hexahydropyrene (HHP) can be interpreted in rational structural terms and illustrates how the mass distribution and configuration of these ion groups is a function of the type of benzylic methylene functionalities present.

EXPERIMENTAL

Wilcox seam lignite (Martin Lake, Texas) is agitated with sonication in ten times its mass of DMSO for twenty four hours, filtered through a ceramic frit, and the solvent removed by evaporation in vacuo. The tar is digested in THF for twenty four hours and the DMSO-soluble, THF-insoluble solid is removed by filtration. Solvent-free THF-soluble matter is digested in excess hexane. Solids are filtered through a ceramic thimble and extracted with hexane in a Soxhlet apparatus for six hours, then with water for twenty four hours, to remove any DMSO. Upon drying, a five percent yield (DAF basis) of asphaltene-preasphaltene blend is obtained in the form of a fine brown powder.

Liquefaction of Herron seam bituminous coal (Illinois No. 6), Pittsburgh seam bituminous coal (West Virginia) and Wilcox seam lignite (Texas) is carried out in tetralin under hydrogen at 400° C. THF-soluble matter is digested in benzene and filtered to obtain preasphaltenes. Benzene-soluble matter is extracted with hexane to yield oil-free asphaltenes.

CFPDMS spectra are taken by methods described previously (9,10).

CFPDMS SPECTRAL RESULTS

The periodic positive ion groups in the mass range 150 to 400 amu are commonly seen in the CFPDMS spectra of coal derived asphaltenes and preasphaltenes. Representative examples are shown in Figure 1. The groups occur with a mass periodicity of from 12.1 to 14.1 amu, and are most apparent in the region from 200 to 350 amu. Mass centroids of these groups are very nearly the same in all samples examined, including the pure hydroaromatic compounds. Average masses of these centroids are listed in Table 2. These masses are very similar to those of analogous FIMS ions obtained from other coal products (7,8). It is significant that these ion groups usually appear at the top of a broad envelope of ions extending from 200 to 500 amu, the high mass downward slope of which is devoid of ion groups. An additional analogy with the FIMS coal spectra is the more intense ion groups below 200 amu. The composite ions could be interpreted as several families of compound group classes of the form $C_nH_{2n-z}O_y$, the populations of which result in apparent mass periodicities of less than fourteen. The CFPDMS spectra of pure hydroaromatic compounds suggests that an alternate explanation must be considered

Figure 2 shows the 150 to 500 amu range of the positive ion CFPDMS spectrum of HHP (MW 208). Fourteen ion groups appear between 152 and 340 amu. The first five groups are large, consisting of the parent ions and its fragments. Higher mass ions are smaller, and from expansions of the spectrum (Figure 2) it is apparent that the ion groups fall at approximatly the same masses as the asphaltene ions (Table 2). The parent ion group (200-208 amu) consists of a benzyl cation type ion at 207 amu, its unsaturated analogs at 205 and 203 amu, and the pyrene cation radical at 202 amu. Most probable structures are shown in Table 1. The latter ions are derived by facile dehydrogenation, for which hydroaromatic compounds are well known (2). Ion groups at lower masses correspond to the extrusion of carbon and hydrogen from the skeleton, as methylene, methine or carbon chains. Fragment masses imply that the extrusions are accompanied by rearrangement, dehydrogenation and/or intramolecular recombination to produce ions isomeric with the most probable structures shown in Table 1. The apparent periodicity of these ion groups is nearly the same as that of the asphaltene ion groups. The smaller "postparent" ion groups - eight of them between 221 and 325 amu - appear to be recombinant ions, originating from the attack of fragment ions on the parent molecule, or on other fragments.

DISCUSSION

In a preliminary survey of the CFPDMS fragmentation behavior of coal-like compounds (6) we have screened polynuclear aromatic hydrocarbons, aromatic and aliphatic carboxylic acids, phenols, aryl ethers, monoalkylbenzenes and hydroaromatic compounds. Oxygen containing compounds invariably yield parent ions an order of magnitude more intense than their fragment ions. Hydrocarbons, such as phenyl pentadecane, dibenzanthracene and hexahydropyrene, do not fragment in this manner, but give rise to fragment ions typically half as intense as the parent ions. The periodicity of the fragment ions is rational, but quite different from that seen in electron impact ionization mass spectrometry. For example, the positive ion CFPDMS spectrum of behenic acid exhibits a series of ion groups of periodicity 14 amu (Figure 3), reflecting random cleavage along the alkyl chain (11). 1,2,5,6 Dibenzanthracene displays fragments of periodicity 13 amu (Figure 3) corresponding to successive expulsion of from one to eight methine groups from the parent structure. The fragment periodicity of alkylaromatics(including hydroaromatic compounds) is not so regular, and their intensities are of the same magnitude as the parent ions. This is a result of multiple fragmentation modes available to benzylic functionalities, and the formation of very stable benzyl cation structures, exemplefied by the fragment ions of HHP shown in Table 1.

CFPDMS fragmentation resembles that of Pyrolysis-Field Desorption Mass Spectrometry (PFDMS). The PFDMS positive ion groups of German coals (8) fall at the same masses as those shown in Table 2. Schulten attributes some of the principal ions of these groups to several series of compositions C_nH_{2n-z}. An additional similarity between PFDMS and

CFPDMS is the appearance of high molecular weight ions of periodicity 74 amu. We find that monoalkylbenzene compounds, and some coal fractions, show positive CFPDMS ions at m/z = 948 + 74 n , where n is 0 to 14. Such ions appear to be polymeric tris-fused triphenylene structures formed in the pyrolytic environment in which the ions are devolatilized (6). Ions of these same masses have also been seen in Schulten's study (8).

The coincidence of the masses of the asphaltene ions with those of HHP and other hydroaromatics leads us to conclude that the CFPDMS technique is detecting hydroaromatic and other benzylic functionalities among the disparate coal components. A supporting observation is the presence of smaller recombinant ions in the spectrum of HHP which appear at masses above that of the parent. This is a general feature of the CFPDMS spectra of hydroaromatic compounds. In the asphaltene spectra, individual recombinant ions are not seen. The variety of hydroaromatics in the sample gives rise to a broad envelope of ions, superimposed by the larger fragment ions. The feature is very obvious in the FIMS spectra (12) of coal liquids. The configuration of the individual ion groups contains information reflecting the population of extant hydroaromatic molecules.

Organic CFPDMS ions have been detected up to 1200 amu in many coal derived products, yet the ion groups described in this report do not appear at masses above 600 amu. These ion groups have not been detected in the CFPDMS spectra of hexane-soluble coal products, because many other intense ions interfere. They are definitly absent from the CFPDMS spectra of DMSO-soluble, THF-insoluble fractions. A working hypothesis is that as hydroaromatic components condense into high molecular weight crosslinked molecules during coalification metamorphosis, their benzylic character is lost.

ACKNOWLEDGEMENTS

Support from the Gas Research Institute, the Robert A. Welch Foundation, and the Center for Energy and Mineral Resources is gratefully acknowledged.

REFERENCES

1 Derbyshire, F. J.; Varghese, P. and Whitehurst, D. D. "Synergistic Effect between Light and Heavy Solvent Components during Coal Liquefaction": Fuel 61, 859 (1982)

2 Stephens, H. P. and Chapman, R. N. "The Kinetics of Catalytic Hydrogenation of Pyrene - Implications for Direct Coal Liquefaction Processing": Preprints Amer. Chem. Soc. Div. of Fuel Chem. 28 (5), 161 (1983)

3 Mochida, I.; Tamaru, K.; Korai, Y.; Fujitsu, H. and Takashita, K. "Carbonization Properties of Hydrogenated Aromatic Hydrocarbons - III Modifying Activities of Hydrogenated Pyrene and its Oxidized Derivitives in the Co-carbonization of Coals and Coal Liquids": Carbon 21 (1), 535 (1983)

4 Weinberg, V. A. and Yen, T. F. "Mesophase Formation in Coal Liquid Solvent Fractions": Carbon 21 (1), 39 (1983)
5 Institute of Gas Technology "Coal Gasification Support Studies Subtask 1-1, Effect of Process Variables on the Initial Coal Gasification Reactions": Final Report, DOE/MC/14705-T5, May 1982
6 Zingaro, R. A.; Macfarlane, R. D. and Zoeller, J. H., Jr. "Application of Unconventional Solvents and Cf-252 Plasma Desorption Mass Spectrometry in Studies of Coal": Annual Report to the Gas Research Institute, March 1984
7 Bodusynski, M. M.; Hurtubise, R. J. and Silver, H. F. "Relationship between Solvent-Derived and Compound-Class Fractions in Coal Derived Distillates and Vacuum Still Bottoms": Fuel 63(1), 93 (1984)
8 Schulten, H-F "Pyrolysis-Field Desorption Mass Spectrometry of Coal": Fuel 61, 670 (1982)
9 Macfarlane, R. D. "Californium-252 Plasma Desorption Mass Spectrometry, Large Molecules, Software, and the Essence of Time": Anal. Chem. 55(12), 1247A (1983)
10 Macfarlane, R. D. and Torgerson, D. F. "Californium-252 Plasma Desorption Mass Spectrometry": Science 191, 920 (1976)
11 Zingaro, R. A.; Vindiola, A. G. and Zoeller, J. H. , Jr. "Fragmentation in Cf-252 Plasma Desorption Mass Spectrometry 1. Positive Ions of Behenic Acid": Int. J. Mass. Spectrom. Ion Phys. 53, 349 (1983)
12 Chen, C-H B. and Durai-Swami, K. "Characterization of Controlled Flash Pyrolysis Coal Liquids": Preprints Amer. Chem. Soc. Div. Fuel Chem. 27 (3-4), 292 (1982)

Table 1: Most probable structures of the main positive CFPDMS fragment ions of 1,2,3,6,7,8 Hexahydropyrene, shown in Figure 2

MASS		MASS	
207		179	
205		178	
203		176	
202		165	
191		163	
189		152	

Table 2: Mean mass centroids of CFPDMS positive ion groups exhibited by asphaltenes and hexahydropyrene in the mass range 150 to 370 amu.

151	224	299
167	237	311
179	250	323
191	263	337
201	275 (irregular)	349
212	284	361

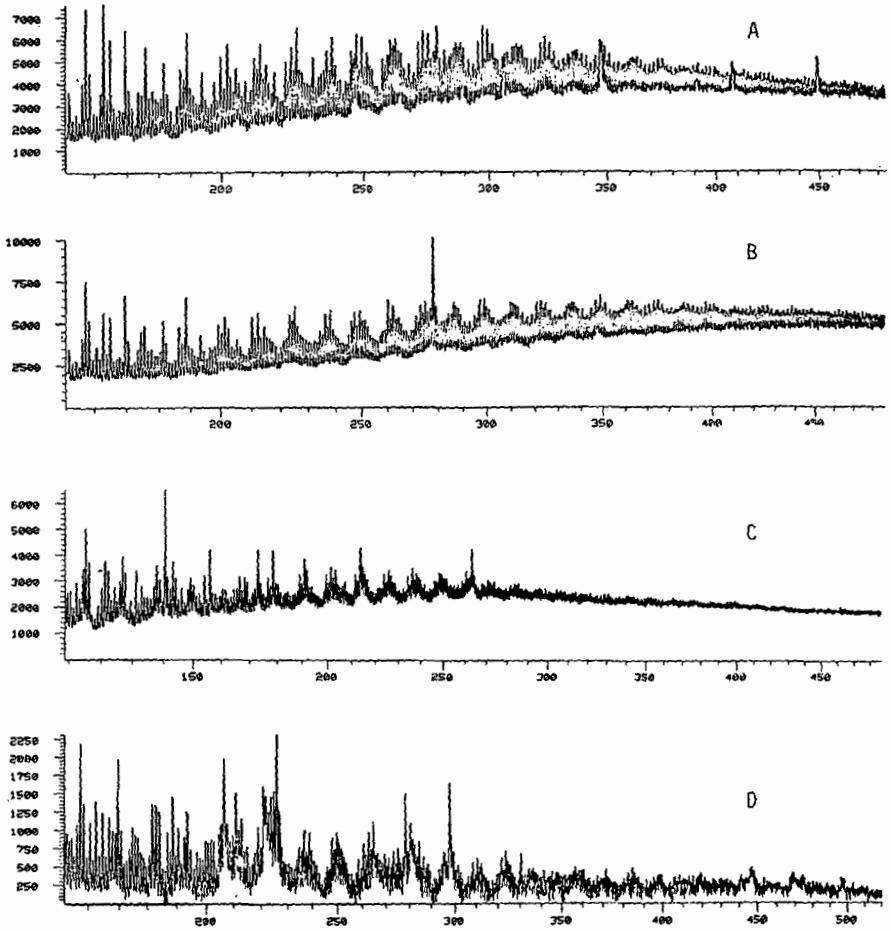

Figure 1: Positive CFPDMS ion groups of Coal derived Asphaltenes in the mass range 150 to 500 amu. A - Illinois No. 6 liquefaction asphaltene, B - Pittsburgh Seam Bituminous Coal liquefaction asphaltene, C - Wilcox Seam Lignite, native asphaltene-pre-asphaltene blend, D - Wilcox Seam Lignite liquefaction preasphaltene.

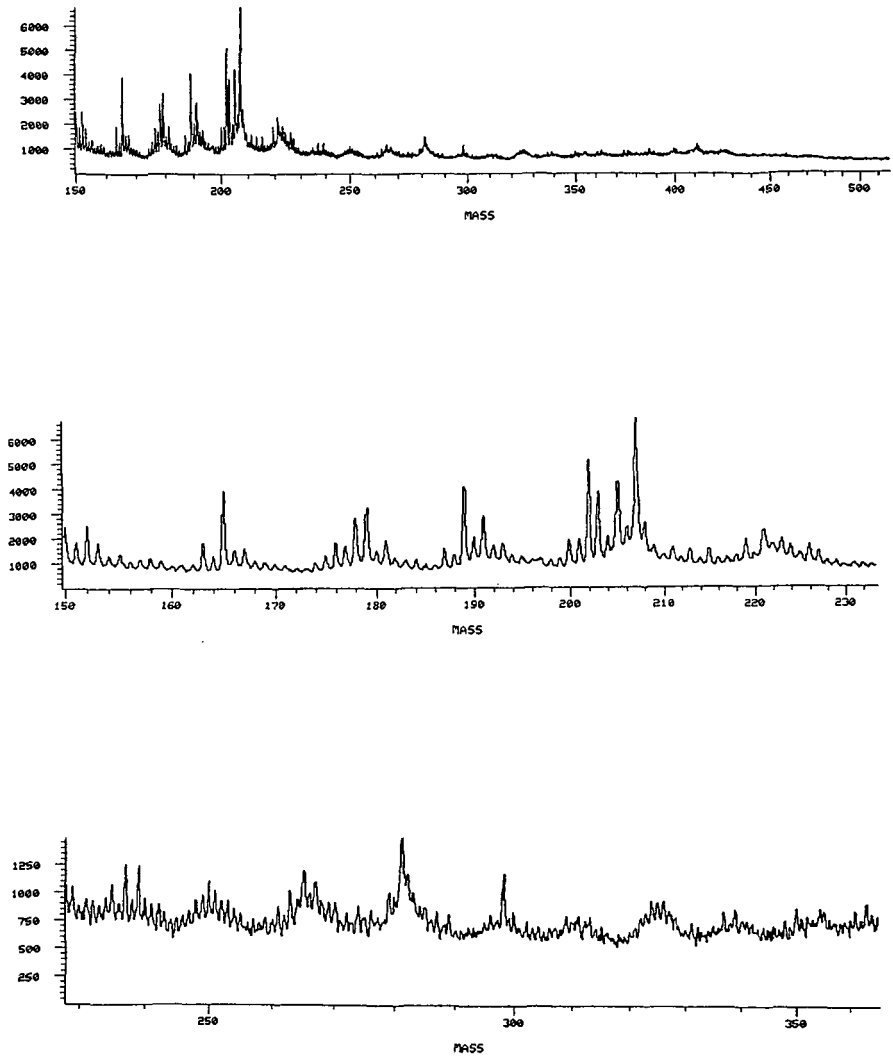

Figure 2: Positive ion CFPDMS spectrum of 1,2,3,6,7,8 Hexahydro-pyrene in the mass range 150 to 500 amu. Vignetts show detail of fragment ions (150 to 208 amu) and recombinant ions (220 to 340 amu).

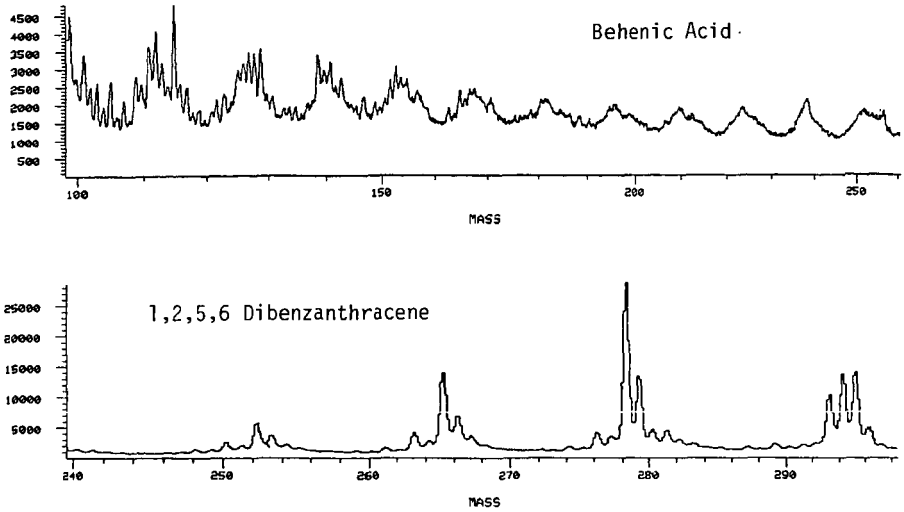

Figure 3: Periodic positive CFPDMS ion groups. Periodicity 14 amu fragments from cleavage of alkyl chain of Behenic acid (Top), and periodicity 13 amu methine extrusion fragments of Dibenzanthracene (Bottom). The Dibenzanthracene spectrum shows the parent ion at 278 amu and an oxygenated impurity at 294 amu.

CHANGES IN ASPHALTENES AND PREASPHALTENES WITH REACTION CONDITIONS AND EFFECTS ON COAL STRUCTURE

C.L. Knudson, R.J. Baltisberger, N.F. Woolsey, and W.G. Willson

University of North Dakota Energy Research Center
Box 8213, University Station
Grand Forks, North Dakota 58202

Asphaltenes (A) and preasphaltenes (PA) have broad chemical compositions because they are solubility fractions. Detailed separations by Baltisberger, et al. (1) of the A and PA fractions and detailed analyses (over 100) of samples produced at 12 different liquefaction conditions have provided a better definition of what chemical parameters most affect their solubility. Relating the A and PA changes to coal liquefaction operating conditions indicates that a key factor in upgrading these materials is to decrease their phenolic content. The changes in hydrogen content and distribution in asphaltenes observed when operating with H_2 or CO-H_2 (syngas) indicated CO was more effective in hydrogenating aliphatic positions in asphaltenes than H_2 gas. The change in hydrogen distribution has implications concerning coal structure (both lignites and bituminous coals) and initial coal decomposition mechanisms.

Experimental

The continuous process unit (CPU) used to produce the A and PA material has been described elsewhere (2). The A and PA fractions were separated from samples obtained from twelve different continuous process unit (CPU) tests performed at the University of North Dakota Energy Research Center (UNDERC). Nine tests were made with Beulah (B3) lignite, one with Big Brown (BB1) Gulf Coast lignite, and two with Powhattan (POW1) bituminous coal. Five tests were single-pass with coal and solvent; three of these five tests were at 400°, 440° and 460°C operating temperatures and a gas flow rate of 0.5 scfm of syngas using a continuous stirred tank reactor (CSTR) while two were at gas flow rates of 0.5 and 1.1 scfm at 460°C using an open tubular reactor. Seven tests were bottoms recycle tests at nominally 460°C and at operating pressures of 2000 to 4000 psi. Operating conditions have been previously reported (1). During CPU operation, a coal-solvent slurry (preheated to 200°C) and reducing gas (preheated to 300°C) was fed to a continuous stirred tank reactor (CSTR) or an up flow open tubular reactor (OTR). Thus, most of the heating to reaction temperatures occurred in the reactor. The redistribution of the feed to product streams is depicted in Figure 1. All streams were sampled after each bottoms recycle pass (4 h) or single pass test period (6 to 12 h) and extensively analyzed. In single pass operation a 40% coal and solvent slurry was passed once through the system. In bottoms recycle, the major portion of product slurry (PS) and usually the light oils (LO) were recycled as solvent for the next pass. Total insolubles including ash and insoluble organic matter (IOM) increase. These remain nearly constant after about ten passes due to the removal of PS not required for use as solvent. The amount of coal fed was 30 wt% of the feed slurry (FS). Only product slurry analyses will be considered in this paper.

Product Slurry Analysis. Product slurry was collected in a 1 gallon can during the last hour of a test period or pass. The contents of the can were shaken in a paint mixer (single pass) or transferred to a Waring blender and blended (bottoms recycle). After mixing, the material was rapidly split into small sample containers and the remainder returned to storage. Settling was not a problem except when distillate solvents were employed in a single pass run. The validity of analysis techniques using microgram quantities was verified by repeated analyses. Samples

were analyzed in duplicate or triplicate to define major product fractions. Water was usually 1% to 3% of the PS and was determined by Karl Fischer titration. Tetrahydrofuran (THF) insolubles were determined by dissolution of a sample in excess THF at ambient conditions and filtration through a 0.5 micron, Teflon, Millipore filter. Distillation residue (MDR) was determined by microdistillation of less than 0.5g at 250°C, 1 Torr for 0.5 h. Ash was determined by initially driving off volatile organics at about 200°C followed by ashing at over 800°C in a muffle furnace. The THF soluble portion of the MDR defined the soluble residue (SR) yield. The quality of the SR was routinely determined by high pressure liquid chromatography (HPLC) gel permeation chromatography (GPC) of the THF soluble fraction of the MDR (3). GPC provided the molecular weight (MW) distribution profile of the SR. Also, the GPC ratio of the absorbance at 254 nm of the exclusion peak or shoulder near 950 MW to the absorbance at 250 MW provided an index value to the amount of high MW material in the SR.

Asphaltenes. The product slurry stream samples were separated into A and PA fractions by exhaustive extraction using toluene and THF. Then each fraction was separated by molecular weight (MW) using Bio Beads -Sx-3 into narrower MW fractions (1). The MW fractions were each analyzed for carbon, hydrogen, nitrogen, sulfur, and phenolic hydroxyl (OH) content. The average MW was determined by vapor phase osmometry. Proton NMR analyses were performed to determine the hydrogen distribution as:

H_{ar} - hydrogens attached to aromatic carbon atoms,
H_a - hydrogens attached to carbons which are attached to an aromatic ring (benzylic hydrogen), and
H_o - hydrogen on carbon at least one carbon atom away from an aromatic ring or in an alphatic hydrocarbon (aliphatic hydrogen).

Single Pass Solvents. The CPU once through tests with the CSTR used an anthracene oil (AO1) purchased from Crowley Tar Products spiked with 10% tetralin while tests with the OTR used AOD1 solvent, which was a distillate fraction of AO1. The solvent analyses have been presented elsewhere (4, 5). Neither AO1 or AOD1 solvent contained any THF insolubles and would therefore not interfere with the preasphaltene analysis unless incorporated into that fraction during processing. The amount of hexane insolubles in the single pass solvents was only 1.28 wt%. In addition, this portion showed a uniform low absorbance value from 2000 to 100 g/mole as indicated in Figure 2. Assuming the low absorbance is consistent with a small concentration there should be no major contribution to the average molecular weight determined by VPO analysis of the asphaltene fractions of the SR samples.

The MDR of AO1 amounted to 8.05 wt% and was entirely soluble in THF. The GPC MW distribution of this material was bell shaped (Figure 2) with minimum values at 950 and 250 MW and therefore would have little influence on the GPC ratio determined for an SR.

Results

Coal Analysis and Reactions. Ultimate and Fischer-Schroeder Assay data (provided by the Alberta Research Council) for the coals are presented in Table I. The 18 to 21 maf wt% oxygen content of the lignites was considerably higher than the 8.6 value for the bituminoua coal. For the B3 lignite about 74% of the total sulfur was retained in the ash as sulfate due to its high molar Ca/S ratio. This increased the apparent ash resulting in the calculated maf oxygen value being low. POW1 and BB1 exhibited sulfur retention of 5% and 84%, respectively. Ignoring the effects of sulfur retention, most of the oxygen in the B3 lignite was observed during 500°C assay as CO_2 and chemical water (51% and 37% for B3, respectively). For the bituminous coal, 58% of the oxygen was observed in chemical water and only 22% in CO_2. Chemical water is water produced in excess of coal moisture (cf. Table I). Typical values depending on rank have been reported for many coals (6). For 200g of

Table I. Coal Analysis

A. Elemental

Rank	Coal[a]	Moisture %AR	Ash %MF	Ultimate, wt% maf C	H	N	O	S
Lig	B3	28.90	16.32	70.10	34.50	1.04	21.60	2 76
Lig	BB1	26.51	12.57	74.05	5.42	1.32	18.09	1.11
Bit	POW1	4.80	10.61	79.96	5.74	1.39	8.59	4.31

B. Fischer-Schroeder Assay Yields, wt% maf[b,c]

Coal	Char	Total Gas	Chemical Water[d]	Tar	Light Oil
B3	66.41	18.85	8.95	4.65	1.83
BB1	63.03	16.25	8.71	9.83	1.04
POW1	69.56	7.97	5.62	15.74	0.12

Coal	Gas	H_2	CO	CO_2	H_2S	C_1-C_6	CH_4	C_2H_6
B3	18.85	0.07	1.49	15.23	0.38	1.61	0.92	0.18
BB1	16.25	0.05	1.79	11.83	0.23	2.34	1.19	0.28
POW1	7.97	0.05	0.52	1.68	1.10	4.54	2.52	0.70

[a]Dry pyritic sulfur contents were 0.63, 0.16, and 0.91, respectively.
[b]Analyses provided by the Alberta Research Council Canada, M. Selucky and M.P. duPlessis.
[c]Dry ash values were 16.75, 11.35, and 10.00, respectively.
[d]Water produced in excess coal moisture under pyrolysis conditions.

B3 coal, CO_2 evolved rapidly prior to reaching 400°C in batch autoclave tests with coal only (7). Similar rates of chemical water and CO_2 production from this coal at various temperatures was observed by Solomon (7). In coal-CO-water-solvent autoclave tests rapid CO_2 production initiated at about 360°C coincident with CO consumption and some H_2 production (8, 9). However, in slurry dried coal CO tests CO_2 was observed with CO consumption but minimal H_2 gas was observed. In rapid heat up tests with about 150g of maf lignite (triple the normal amount) to 3 moles of CO, 98% of the CO was rapidly converted to CO_2. The amount of CO consumed was found to be proportional to the amount of coal charged.

In continuous process unit operation at the UNDERC with H_2 gas, the water and CO_2 yields are similar to the assay CO_2 and chemical water yields of the coal being processed. When CO gas was present the molar amount of CO consumed approximated the quantity of feed water (coal moisture plus chemical water) consumed. In summary, the chemical water was produced rapidly at temperatures above 360°C without consuming gaseous hydrogen but rather abstraction of coal hydrogen which reduces the net available hydrogen in the coal. Loss of this hydrogen in chemical water would increase aromatization during the initial coal reactions. This net available hydrogen has been found to correlate with liquefaction conversion and pyrolysis tar yields (10). The CO results indicated that CO reacted with the chemical water or

its functional group precursor to result in the net hydrogenation of the coal structure. This necessitates the presence in coal of functional groups that can thermally decompose to produce water at temperatures as low as 360°C.

Temperature Effects - Single Pass CPU Runs. The reaction temperature has a large effect on the characteristics of the SR, PA, and A fractions and on yield structures. Conversion values of coal increased with temperatures from 400° to 460°C but decreased at 480°C for these tests. The yield results at 480°C are solvent dependent. The SR fraction exhibited a rapid and then slower decrease in over 950 MW material with increasing temperature (Figure 3) as was observed in batch autoclave tests (3). The preasphaltene fraction indicated a similar decrease in the magnitude of the exclusion peak with temperature (Figure 4). The individual PA-MW fractions all exhibited uniformly decreased hydrogen content with increasing temperature as seen in Figure 5. The range of molecular weights for the PA-MW fractions compressed from 200-3000 to 400-2000 to 500-1000 with increasing temperature (see Figure 5). This indicated that the PA material became more refractory 500-1000 MW material through the loss of lower MW material. Solvent incorporation into the lower MW PA could also result in an upward shift in MW especially at 480°C since at this temperature coal conversion decreased relative to conversion at lower temperatures.

The A-MW fractions (not depicted) obtained at 480°C had higher hydrogen content than those obtained at 460°C indicating that hydrogen rich solvent had been incorporated. The phenolic contents of both A- and PA-MW fractions obtained at 400°C changed in a parallel manner but were higher than those obtained at 460°C and 480°C. The exception was the 460°C PA-MW fractions which were even higher then the values obtained at 400°C.

Pressure Effects During Bottoms Recycle. The relationship of A and PA material can be better understood by consideration of the effects of pressure on their hydrogen and phenolic OH content. Figure 6 presents the data for the hydrogen content changes with MW for the A- and PA-MW fractions of the bottoms recycle Runs 46 and 41 at 2000 and 4000 psi, respectively. The hydrogen content of both the A- and PA-MW fractions increased at any particular MW for the higher pressure indicating the greater hydrogenation which occurs at higher pressures was similar for both A and PA material. The OH content of the PA-MW fractions was higher and parallel to those of the A-MW fractions. However, as seen in Figure 7, the OH content for the PA-MW fractions of the same MW was higher when operating at 4000 psi than at 2000 psi (the A-MW fractions behaved similarly with pressure). The higher operating pressure increased the hydrogen content, as well as the phenolic content. At higher pressures the yield structure changed, as indicated in Figure 8. At 4000 psi operation, insoluble organic matter (IOM) was less (conversion was higher), and the amounts of A and PA produced were less than at 2000 psi operation. However, increased conversion due to increased operating pressure resulted in producing A and PA that had a higher OH content. The molecular weight distribution of the SR was also higher when operating at 4000 than at 2000 psi. The phenolic content of distillates also increased with conversion (12). The higher operating pressure increased 1) conversion, 2) the hydrogen content of the A and PA, 3) the phenolic content of the A and PA, and 4) the GPC molecular weight distribution of the SR fraction.

Effect of CO on Hydrogenation of Lignite and Bituminous Coal. The influence of CO on the hydrogenation of asphaltenes derived from lignite or bituminous coal indicated that CO preferentially hydrogenated the H_o position. Table II presents the operating conditions, conversions, and SR yields for four bottoms recycle tests with and without CO for two coals. CO-H_2 was somewhat more effective at converting lignite while H_2 was more effective for converting bituminous coal. SR yields also varied. The GPC-MW distributions were essentially identical for the two coals when

Table II. Effect of CO on the Hydrogenation of Asphaltenes

Coal	Lignite, B3		Bituminous, POW1	
CPU Run[a]	41	45A	69	53
Feed Gas	$CO-H_2$	H_2	$CO-H_2$	H_2
Total Pressure, psi	3841	1990	2633	2006
Partial Pressure, pH_2	1563	1707	1225	1907
pCO	1604	--	1291	--
pH_2O	600	270	71	98
pLO	58	13	47	0
Flow Rates:				
Feed Gas, scfh	44	55	38	32
Feed Slurry, kg/h	2.18	2.28	2.47	2.36
Ratio, PS/FS[b]	0.782	0.793	0.787	0.832
Yield, wt% maf coal:				
Conversion	92	88	87	92
SR	21	14	22	16
Asphaltene	12.0	10.5	15.6	--
Preasphaltene	6.0	5.5	6.3	--
Ratio PS/FS[c] H/C	0.996	1.022	0.981	1.028
Light Oil H/C	1.503	1.602	1.420	1.473
Asphaltenes:				
VPO MW, g/mol	372	384	347	336
H/C	0.911	0.865	0.809	0.765
% H_{ar}	37.4	43.8	48.9	54.5
% H_a	34.1	35.4	31.7	30.0
% H_o	26.1	18.3	17.8	13.7
% H_{OH}	2.4	2.5	1.6	1.8
Preasphaltenes:				
VPO MW, g/mol	671	676	702	701
H/C	0.727	0.740	0.636	0.676
% H_{ar}	43.5	43.3	52.1	53.9
% H_a	28.3	29.2	23.9	23.3
% H_o	24.7	23.4	21.6	19.6
% H_{OH}	3.5	3.4	2.4	3.2

[a]CPU bottoms recycle operation with light oil add back except in Run 52. The light oil partial pressure in the gas phase is expressed by pLO.

[b]The ratio of flow rate of the product slurry (PS) to the feed slurry (FS).

[c]The ratio of the H/C ratio of the product slurry to that of the feed slurry.

only H_2 gas was present. When the same start up solvent was used, the MW distribution of the SR was distinctly lower over the entire run when operating with CO than without CO and seen in the B3 runs.

The partial pressures of hydrogen were higher in the runs that used H_2 gas. This resulted in greater over all hydrogenation as indicated by somewhat higher H/C values for the light oil product and for the ratios of the (H/C ratio of the product slurry) to the (H/C ratio of the feed slurry). The A and PA data on Table II indicate great similarities when operating with and without CO except when comparing the H content and the hydrogen distribution of the asphaltenes. The asphaltene fraction from each coal showed a significant increase in the H content (also the H/C ratio) and in the H_o (aliphatic hydrogen) content when CO was used. The preasphaltenes had slightly lower H content but were slightly higher in H_o content. These results indicate a tangible benefit to the presence of CO on the hydrogenation of the asphaltene fraction.

Conclusions

Asphaltene and preasphaltene data have been presented to demonstrate the effect of temperature, pressure, and reducing gas composition on their hydrogen and phenolic content. The previous paper by Baltisberger (1) showed how the hydrogen and phenolic content of the A and PA defined whether or not a coal derived product will be classified as such. The influence of processing parameters as discussed in this paper indicates that reduction in the number of phenolic functional groups and cracking are required to further convert asphaltene and preasphaltene material to distillates.

The influence of CO on the H_o positions of asphaltene along with the previously discussed data on CO and water reactions has a significant effect on models postulated for the original coal structure and on possible initial steps in coal decomposition. Large numbers of hydroxyl functional groups must be present in the coal which will decompose to water as low as 360°C. However, the hydroxyl groups must be primarily in aliphatics or alkyl side chains on aromatics to satisfy the increase in H_o observed in reactions where CO was present. This suggests that a dewatering reaction occurs thermally (with or without H_2 gas) as indicated in Equation 1.

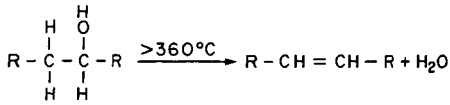

1)

Some phenolic functional groups may also decompose to water. However, hydrogenation at this position would not result in an increase in H_o content.

With carbon monoxide present, the overall reaction to hydrogenate the coal structure (without observing H_2 gas and less water products) would occur as in Equation 2.

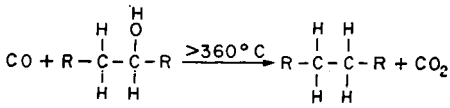

2)

The R-groups would need to activate dewatering since typical alcohols such as cyclohexanol do not decompose thermally to cyclohexene at 375°C (13). Glycols such as those found in cellulose, do decompose to water at about 360°C (14). Coal models

do not include water producing functional groups (15,16). However, these models were prepared to represent a coal model that would predict observed products (17) and are valid for reactions in H_2 gas. Also, cellulose is reported to decompose and therefore is considered to be absent. Indeed, only 0.01% cellulose was obtained by the direct extraction of a Beulah lignite (18). The presence of humic acids in coals is well documented (19). However, residual fragments of cellulose or humic acids incorporated into the coal structure may account for the presence of alcohol functional groups.

That alcohol groups are present in aromatic bridging structures was indicated in the data in this report by the decreased MW of SR when processed with CO present since after hydrogenation an aliphatic bridge would cleave easier. The rapid thermal cleavage of biphenylethane (bibenzyl) relative to the stability of biphenylethylene at liquefaction temperatures (20) is an analogous situation. The increased aliphatic hydrogen content in the asphaltene fraction when reacted with CO may also indicate that some alcohol groups were initially in the aromatic bridges. The presence of alcohol groups in long chain aliphatics has been indicated because increased yields of long chain alkanes were observed when CO was present (12).

In conclusion, the previous data has shown how operating conditions such as pressure and temperature affects the hydrogen content, phenolic content, and molecular weight range of asphaltene and preasphaltene fractions. The effects are reflected similarly in individual MW fractions of both A and PA material. The presence of alcohol groups in original coal (both lignites and bituminous coals) was strongly suggested. The preferential reaction of these alcohol groups with CO gas (but not H_2) to increase the hydrogen content of the asphaltenes, to reduce the overall MW distribution of coal, and to increase yields of alkanes indicates the beneficial effects of CO as a reductant of these functional groups which are present in both lignites and bituminous coals.

Acknowledgments

This work was performed at the University of North Dakota Energy Research Center, formerly the Grand Forks Energy Technology Center of DOE. This paper was prepared under Cooperative Agreement No. DE-FC21-83FE60181 for the U.S. Department of Energy, Office of Fossil Energy, Morgantown Energy Technology Center and the Grand Forks Project Office.

Literature Cited

1. Baltisberger, R.J.; Woolsey, N.F.; ACS Div. of Fuel Chem. Preprints, 1984, Aug. (submitted).
2. Willson, W.G.; Knudson, C.L.; Baker, G.G.; Farnum, S.; Severson, D.E.; Owens, T.C.; Souby, M. Proc. 1981 Lignite Symposium; San Antonio, June 1981.
3. Kundson, C.L.; Shiller, J.E.; Ruud, A.L. in "Organic Chemistry of Coal"; Larsen, J.W., Ed.; ACS SYMPOSIUM SERIES NO. 71, American Chemical Scoeity: Washington, D.C., August 1977, pp. 301-316.
4. Farnum, S.A.; Farnum, B.W.; Bitzan, E.F.; Willson, W.G.; Baker, G.G. Fuel 1983, 62, 799.
5. Knudson, C.L.; Farnum, B.W., in preparation.
6. Gomez, M.; Goodman, J.B., Bureau of Mines Report of Investigation 5009, 1953.
7. Solomon, P.R.; Hamblen, D.G.; Carangelo, R.M., Report by Advanced Fuel Research, April 22, 1981.
8. Sondreal, E.A.; Knudson, C.L.; Shiller,. J.E.; May, T.H. Proc. 1977 Lignite Symposium; DOE GFFETC/IC-77/1, pp. 129-158.
9. Knudson, C.L.; Willson, W.G.; Baker, G.G. ACS Div. of Fuel Chemistry Preprints, 26(1), 1981, p. 132.
10. Knudson, C.L.; duPlessis, M.P.; in preparation.

11. Willson, W.G.; Knudson, C.L.; Baker, G.G; Owens, T.C.; Severson, D.E., "Application of Liquefaction Process to Low-Rank Coals", Proc. 1979 Lignite Syumposium; Grand Forks, May 1979.
12. Farnum, S.A., private communication.
13. Reddy, P.A.; Stenberg, V.I., submitted.
14. Morita H.; Rice, H.M. Anal. Chem. 1955, 27, 336.
15. Whitehurst, D.D. in "Organic Chemistry of Coal"; Larsen, J.W., Ed.; ACS SYMPOSIUM SERIES NO. 71, American Chemical Society: Washington, D.C., August 1977,pp. 1-36.
16. Sondreal, E.A.; Willson, W.G.; Stenberg, V.I. Fuel 1982, 61, 925.
17. Wiser, W.; private communication, 1981.
18. Olsen, E.; private communication.
19. Fowkes, W.W. "Some Characteistics of Natural and Coal-Derived Humates: with Bibliography", DOE/GFERC/IC-75/1, NTIS, 67 pages.
20. Stenberg, V.I.; Van Buren, R.; Raman, K.; Knudson, C.L., "Process Chemistry of Direct Liquefaction of Lignite with Hydrogen and Carbon Monoxide", Penn State Short Course, June 1981.

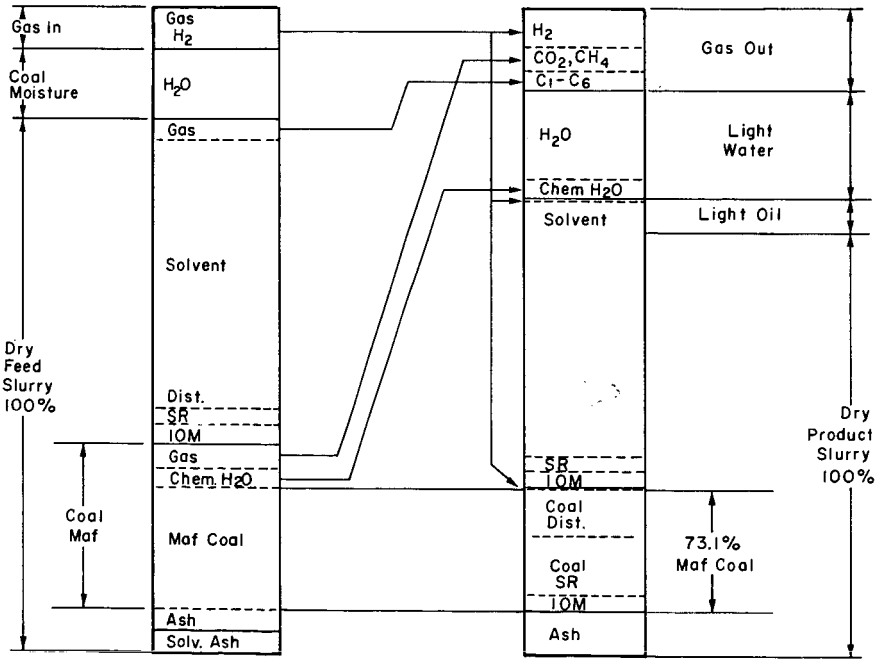

Figure 1. Redistribution of Continuous Process Unit feed streams to product streams.

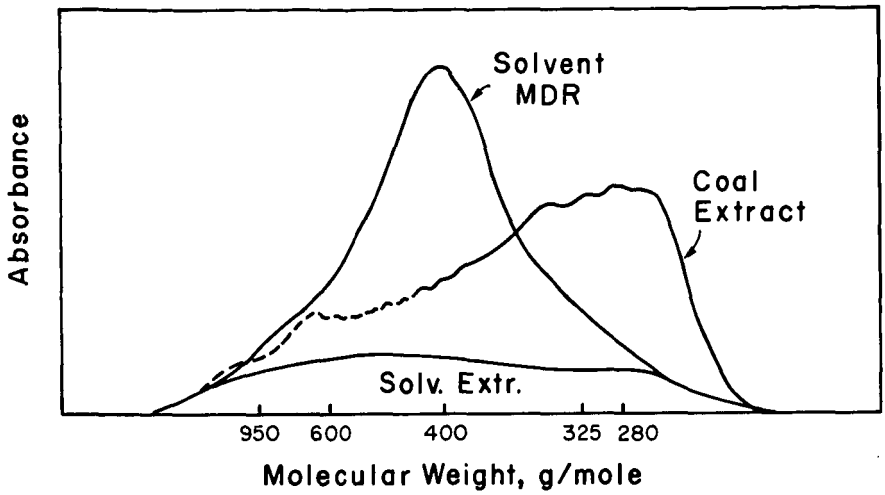

Figure 2. HPLC-GPLC molecular weight distribution of SR (Solvent MDR) and asphaltene fraction (solvent extract) of the solvent A01. Asphaltene extracted from a coal-solvent slurry (coal extract) is also depicted.

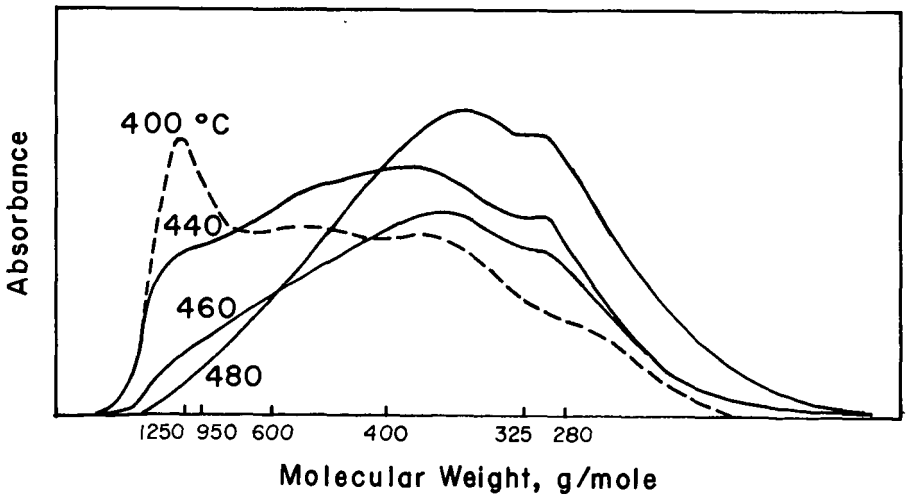

Figure 3. Changes in the MW distribution of SR with CPU operating temperature.

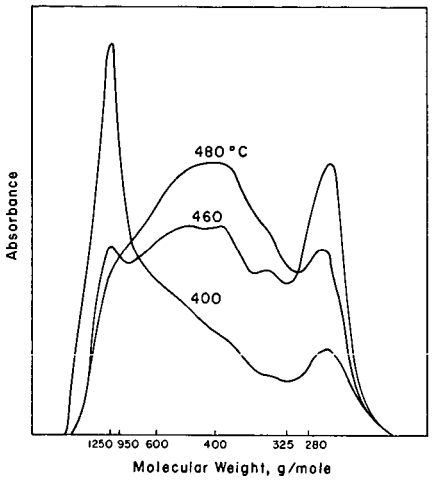

Figure 4. Changes in the MW distribution of the preasphaltenes with CPU operating temperature.

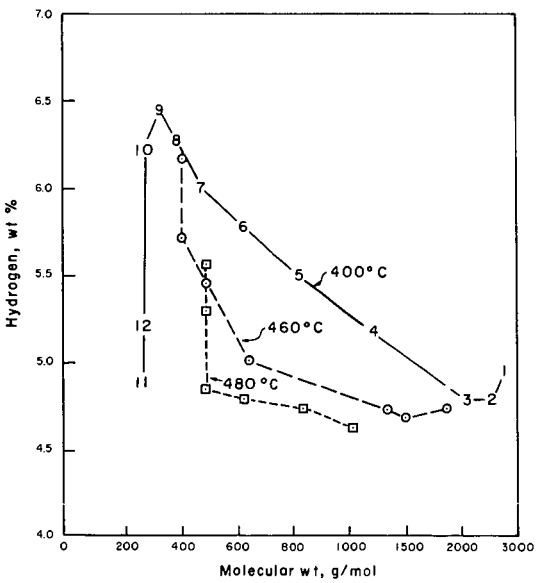

Figure 5. Changes in the hydrogen content of preaaphaltene MW-fractions with CPU operating temperature.

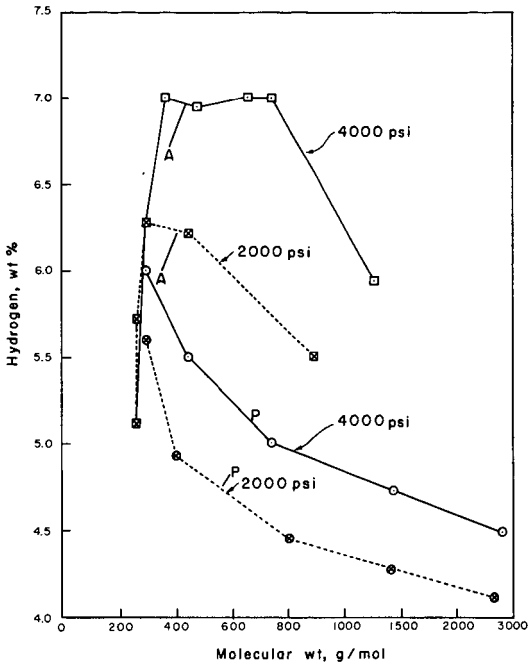

Figure 6. Effect of operating pressure on the hydrogen content of asphaltene and preasphaltene-MW fractions. Data for unseparated samples is indicated by A for asphaltenes (⊡,⊠) and P for preasphaltenes (⊙,⊗).

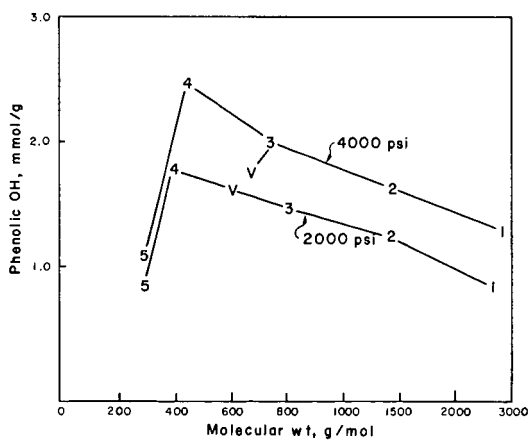

Figure 7. Effect of operating pressure on the OH content of preasphaltene-MW fractions. Unseparated sample data is represented as V.

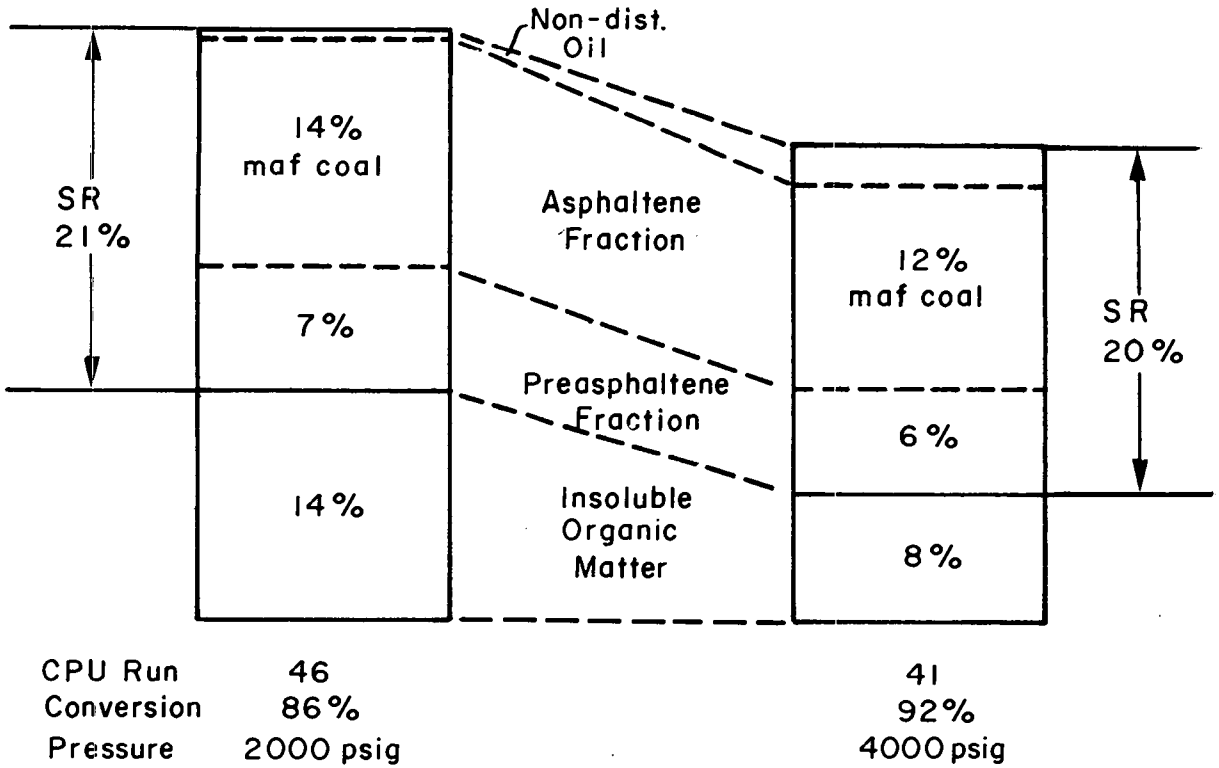

Figure 8. Effect of operating pressure on the yield structure.

SOLUBILITY PARAMETER RELATIONSHIPS BETWEEN LIGNITE DERIVED ASPHALTENES AND PREASPHALTENES

R.J. Baltisberger, N.F. Woolsey, J.F. Schwan, G. Bolton and C.L. Knudson

Department of Chemistry and University of North Dakota Energy Research Center, University of North Dakota, Grand Forks, North Dakota 58201

INTRODUCTION

In addition to the distillable products a sizeable portion of the low rank coal liquefaction products fall into asphaltene and preasphaltene categories. Asphaltenes are generally defined as those components in petroleum or coal liquids which under specific extraction conditions are soluble in benzene or toluene but insoluble in pentane or hexane (1,2). Preasphaltenes are those components that are soluble in pyridine or tetrahydrofuran but are insoluble in benzene or toluene. Farcasiu et al. (3) proposed the name, asphaltols, for this latter class of compounds because of the polyfunctional nature of these materials. In their work it was concluded asphaltenes are primarily monofunctional compounds while preasphaltenes are polyfunctional as determined by comparison of selective elution sequential chromatographic fractions and model compounds using thin layer chromatography (3,4). Preasphaltenes are formed in the initial stages of coal liquefaction where their formation may be responsible for the high viscosity of the products and for other processing difficulties (5). The preasphaltenes, on a weight basis, produce a viscosity about twice that for the asphaltene fraction (5).

Comparison of the structural features of asphaltenes and preasphaltenes show major differences between the two solubility categories occur with (1) their molecular weight distributions, (2) the fraction of total carbon present as aromatic carbons, (3) the fraction of total aromatic carbon present as edge aromatic carbons, (4) the fraction of oxygen present as phenolic and etheral oxygen atoms, and (5) the relative amount of hydrogen to phenolic content based on a per gram of total sample. Of all of these parameters a simple relationship of hydrogen and phenolic oxygen content has been found to establish the solubility of asphaltene and preasphaltene samples. The interrelationship between structural parameters will be discussed in this paper and in a subsequent paper (6) the relationship of these parameters to process conditions will be discussed.

EXPERIMENTAL

Liquefaction samples were obtained from the University of North Dakota Energy Research Center (formerly the Grand Forks Energy Technology Center). The reactor conditions are described in Table 1. The samples were isolated into asphaltene and preasphaltene fractions using exhaustive extraction techniques with toluene and tetrahydrofuran, respectively.

The asphaltene and preasphaltene samples were further separated using a preparative scale GPC column composed of 50 mm id x 120 cm glass column packed with Bio-Beads S-X3 (200-400 mesh) styrene-divinyl benzene copolymer. Prior to GPC separation all samples were acetylated with C-14 labeled acetic anhydride in order to convert all hydroxyl groups to acetate for minimization of hydrogen bonding during GPC fractionation. Elemental analyses were performed to determine elemental composition. Oxygen was determined by difference after

correction for labeled acetate present. The phenolic hydroxyl content was measured by combustion and C-14 counting content of resulting CO_2. Number average molecular weights of the samples were measured using a Model 117 Vapor Pressure Osmometer using pyridine as the solvent at 75°C. In normal runs, 2-3 concentrations over a range of 1 to 50 g/Kg·of pyridine were employed for extrapolation to infinite dilution.

RESULTS AND DISCUSSION

The chemical composition and structural features of a number of over 100 different lignite and bituminous coal liquefaction asphaltene and preasphaltene samples were measured. The overall percentage by weight of the starting coal falling into either the asphaltene or preasphaltene class and conditions of preparation are given in Table 1. In the case of the 15 and 26 series samples insufficient data are available to correct the percentages to a maf basis. The basic analytical data for the asphaltenes and preasphaltenes studied by Baltisberger et. al. (7) are summarized in Table 2. The three most significant structural factors are the molecular weight, oxygen functionality and nature of the aromatic carbons.

A. Solubility Parameter Relationships

The lignite and coal derived products were obtained over a range of temperatures from 400° to 480°C, under hydrogen or hydrogen-carbon monoxide pressures from 1500 to 4000 psi and various donor solvent conditions. The samples were fractionated into asphaltenes and preasphaltenes by solvent extraction using toluene and tetrahydrofuran (THF). The extracts were further fractionated by preparative GPC techniques. The isolated fractions were then analyzed for elemental composition, number average molecular weight by VPO using pyridine as the solvent, hydroxyl oxygen content by acetylation procedures and carbon structure by NMR techniques.

Plots of mole fraction of hydrogen; mole ratio of H/C; mole ratio of H/(C+N+O+S); mole ratio edge aromatic carbons/aromatic carbons, H_{aru}/C_{ar}; or moles hydrogen per 100 g sample were constructed versus the phenolic oxygen content in OH moles/100 g sample or mole fraction of OH. All the plots show a similar differentiation between asphaltenes and preasphaltenes as illustrated in Figure 1 for the moles of hydrogen per 100 g sample. The separation of the asphaltene (87%) and preasphaltene (84%) samples fall into two distinct regions of the graph. The portion of samples that did not fit were primarily low molecular weight preasphaltene and high molecular weight asphaltene samples. This is probably due to imperfections in the solubility separation. For example, part of the asphaltene fractions may have become trapped by adsorption processes in the preasphaltene portions during the extraction process. Steffgen et al. (1) have shown that great care must be taken during the fractionation of oil from asphaltene samples. It would be expected that great care should be exercised during the separation of asphaltene and preasphaltene samples. Equation 1 gives the fit for the dividing line added to Figure 1.

$$Z = H\% - (0.486 \pm 0.008)\ \text{OH mmole/g} - (4.47 \pm .02) \qquad (1)$$

Asphaltenes samples lie above the line giving positive Z values while preasphaltene samples give negative values. Samples which fit the wrong category are indicated by an X under the VTRA column of Table 2. The best differentiation occurred for the plot of molar density of moles H/100 g (wt % hydrogen) versus moles OH/100 g. Parameters which include parts of the total

data or terms calculated from parts of the data gave more mixing of the asphaltene and preasphaltene points. The most mixing occurred for H/C (Figure 2) or H_{aru}/C_{ar} (Figure 3) versus moles OH/100 g plots. Less mixing occurred for H/(C+N+O+S) while the best differentiation resulted when moles H/total sample wt were used. Correlation coefficient values (r values) computed using an IBM statistical analysis package are presented in Table 3. Overlap of the distinct regions shown in Figures 1 through 3 increased with the decreasing correlation of the parameter with mole fraction of hydrogen. Phenolic oxygen content have essentially with no linear correlation with hydrogen content for asphaltene samples while preasphaltene samples show some correlation (see Figure 4).

For the dissolution of a compound, A, into a solvent; the molar solubility

$$A(solid) \rightleftarrows A(liq) \qquad (2)$$

of A is a function of the activity coefficient, γ_A, where K° would be the

$$\text{Solubility} = S = \frac{K^\circ}{\gamma_A}$$

thermodynamic solubility constant for equation 1. From solubility parameter theory for regular solutions the activity coefficient, γ_i, for a solute i dissolving into solvent j is given by Equation 3 (8), where δ is the value of the Hildebrand solubility parameter of the solvent or solute and V_i is the

$$RT\ln\gamma_i = V_i(\delta_i-\delta_j)^2 \qquad (3)$$

molar volume of the solute. For maximum solubility the activity coefficient should approach unity and thus it is desirable to have $\delta_i = \delta_j$. The rule of thumb used in organic chemistry is that 'like dissolve like'. The solubility regions defined by Figure 1 suggest that the ordinate, hydrogen to other elements, is a function of the π and dispersive interactions of the coal matter while the abscissa, mmoles OH/g, is a function of the hydrogen bonding. Clearly the total hydrogen and hydroxyl contents are decisive parameters for establishing the benzene or THF solubility of the coal materials.

Equation 3 predicts an increase of the solubility activity coefficient with increasing molar volume of the solute. Several attempts were made to include V_i in the correlations by plotting log (H/C + MW) or log (H/C + MW/10) versus the acidity of the samples. This approach always mixed the asphaltene and preasphaltene regions. Asphaltenes and preasphaltenes have considerable overlapping of the molecular weights although on the average the total preasphaltene sample is several hundred grams/mole higher for the same process. We observed for all series of preasphaltene samples obtained from the same process conditions that the molecular weight increased as the H/C mole ratio decreased (see Figure 4). The molecular weights of each fraction of the preasphaltenes and asphaltenes from runs 46 and 32 are shown on Figure 4 so the overlap of the molecular weight ranges can be observed. Asphaltene samples show that molecular weights are virtually independent of the H/C ratio and that the acidity changes occur in no reproducible way. The major difference shown in Figure 4 is the removal of phenolic oxygen when going to recycle conditions (run 46) as opposed to those without bottoms recycle (run 32). Other oxygen is also lowered by the recycle conditions although this factor is not apparent in

the figure. The molecular weight data for Figure 4 is given in Table 4. This behavior is representative of all the samples when individual runs are compared. Because of the different molecular weight relationships for asphaltene and preasphaltene samples, it is not surprising that molecular weight terms can not correlate directly in the solubility plots such as Figure 1.

Plots of the mole fraction of hydrogen or H_{aru}/C_{ar} versus acidity are not as effective in defining the solubility regions as is the graph of mole fraction hydrogen. A major contributing factor in these correlations is due to the relationship between aromaticity and condensation and the carbon to hydrogen mole ratio. The fraction of aromatic carbons is defined by equation 4

$$f_a = \frac{C/H - (H^*_{al}/2)}{C/H} \tag{4}$$

where C/H is the carbon to hydrogen mole ratio and H^*_{al} is the mole fraction of aliphatic hydrogens in the sample as determined by NMR measurements (9). The condensation is represented by the number of hypothetical edge aromatic carbons (H_{aru}) per total aromatic carbons (C_{ar}) as defined by equation 5,

$$H_{aru}/C_{ar} = \frac{H^*_{ar} + H^*_{al}/2 + (OH + 2\ O)/H}{F_a(C/H)} \tag{5}$$

In equation 5, H^*_{ar} corresponds to the mole fraction of aromatic protons as determined by NMR and the oxygen terms are mole ratios to total hydrogen (9). The magnitude of both f_a and H_{aru}/C_{ar} are determined to a large extent by the C/H ratio. However, the solubility of a molecule must be determined by additional factors as well as the percentage and condensation of the aromatic carbons.

Oxygen comprises 4 to 8% of the sample by weight and is 40 to 70% phenolic depending on the solubility category. Table 5 shows the percentage of oxygen as phenolics and ethers. For most of the recycle samples preasphaltenes contain 40-50% of the oxygen as phenolics while asphaltenes are 60-75% phenolic. On the other hand, non-recycle conditions lead to nearly equal amounts of etheral and phenolic oxygen for both asphaltene and preasphaltene samples. Only the phenolic content of the samples is taken into account in the abscissa. The ether content undoubtedly has an influence on the size, shape and π-π interactions of the aromatic systems. Thus, the inclusion of oxygen content with the ordinate better correlates the dispersive, size, shape and π-π interactions of the molecules. Another factor influencing solubility would be the nature of the aliphatic carbons. Liquefaction under hydrogen alone tends to produce asphaltenes and preasphaltenes with (shorter average aliphatic chain length) than do hydrogen-carbon monoxide systems (10). Lacking inclusion of a specific term for the length of the aliphatic chains, the influence of aliphatic carbons is best taken into account using the total moles of hydrogen in the abscissa. Nitrogen contents are generally small and evenly distributed, except for a sizeable fraction of low MW preasphaltenes that had appreciably higher values. Sulfur contents are also small and both asphaltene and preasphaltene contents appear to respond similarly to processing condition.

CONCLUSIONS

Comparison of the total fractions of the preasphaltenes and asphaltenes of the same process show the following.

First, preasphaltene samples increase in the fraction of aromatic carbons and degree of condensation with increasing molecular weight. Asphaltenes samples, on the other hand, increase in the fraction of aromatic carbons with decreasing molecular weight. The degree of condensation maximizes at high and low molecules weight values.

Second, asphaltene samples have lower f_a and higher H_{aru}/C_{ar} values than the preasphaltenes. Asphaltenes contain fewer condensed aromatic molecules than do the preasphaltenes.

Third, the phenolic acid content is lower for the asphaltene samples in general. This acidic property works in combination with the total hydrogen content to ultimately determine into which solubility category a sample may fall.

Fourth, Table 3 shows that the recycle preasphaltene samples contain a higher percentage of oxygen and much of that is due to increased other (non phenolic) oxygen, possibly in ethers. Recycle asphaltene samples contain about 60-70% phenolic oxygen, while preasphaltenes contain 40-50% phenolic oxygen. Non-recycle conditions lead to higher total oxygen contents of both categories and to nearly the same distribution between asphaltene and preasphaltene samples. Recycling of the vacuum bottom leads to an etheral oxygen removal. This is probably one reason for the success of the plot of mole fraction of total hydrogen versus phenolic content rather than the plot of H_{aru}/C_{ar} versus phenolic content gives a better separation of asphaltene and preasphaltene samples. The mole fraction of the hydrogen term takes in account the oxygen content of the sample further separating the regions of Figure 1.

Fifth, molecular weight ranges of the two categories overlap. When a number of samples within a narrow range was examined, one observed that the majority of the preasphaltenes lie in a range from 600 to 2500 g/mol while the asphaltenes lie between 300 to 600 g/mol. Preasphaltene samples increased in phenolic content with decreasing molecular weight (see Figure 4). Asphaltene samples show random phenolic content with molecular weight. However, inclusion of the molecular weight directly in a solubility plot similar to Figure 1 was not successful.

For the lignite process samples studied, the differentiation of the asphaltene and preasphaltene samples follow equation 1 rather well for over 80% of the samples. Hydrogen and phenolic content seem to be the only parameters needed to specify into which solubility category the hexane insoluble portions (non distillable) of a lignite liquefaction process may lie. The implication is that it is desireable to lower the phenolic oxygen content while raising the H/C mole ratio during liquefaction.

ACKNOWLEDGEMENT

This research was supported by DOE through contract number DE-AB18-78FC02101.

REFERENCES

1. Steffgen, F.W.; Schroeder, K.T.; Bockrath, B.C. Anal. Chem. 1979, 51, 1164-1168. Steffgen, F.W.; Schroeder, K.T.; Bockrath, B.C. ibid, 1979, 51, 1168-1172.
2. Mima, M.J.; Schultz, H.; McKinstry, W.E., In "Analytical Methods for Coal and Coal Products", C. Karr, Ed.; Academic Press: New York, 1978; Vol I, Chapter 19, pp 557-568.
3. Farcasiu, M.; Mitchel, T.O.; Whitehurst, D.D. ACS Fuel Division Preprints 1976, 21 (7), 11-26.
4. Farcasiu, M. Fuel 1977, 56, 9-14.
5. Bockrath, B.C.; LaCount, R.B.; Noceti, R.P. Fuel 1980, 59, 621-626.
6. Knudson, C.L.; Willson, W.G.; Baltisberger, R.J.; Woolsey, N.F. ACS Fuel Division Preprints 1984, 29, following this article.
7. Baltisberger, R.J.; Stenberg, V.I.; Klabunde, K.J.; Woolsey, N.F. Final Report, The Chemistry of Lignite Liquefaction, DOE/FC/02101-23, July, 1983.
8. Karger, B.L.; Snyder, L.R.; Horvath, C. "An Introduction to Separation Science", Chapter Two, Wiley: New York, 1973.
9. Brown, J.K.; Ladner, W.R. Fuel 1960, 39, 87-96.
10. Farnum, S.A. Private communication.

Table 1. Asphaltene and Preasphaltene Yields and Continuous Process Operating Conditions

Sample	Yield, wt % maf Coal Asphaltenes[a]	Preasphaltenes[a]	Conversion	Gas	Gas Flow scfh	Press, Psig	Temp, °C	Coal[b]
Bottoms Recycle Operation[c]								
44-12[d]	9	5.0	92	$CO-H_2$	52	1978	458	B3
46-16[e]	14	7.0	52	$CO-H_2$	52	2013	458	B3
41-14	12	6.0	92	$CO-H_2$	44	3841	459	B3
45-15	10.5	5.5	88	H_2	55	3934	461	B3
58-15	11.3	5.7	95	H_2	41	2651	459	BB2
53-18	NA	NA	92	H_2	32	2006	469	POW1
69-12	15.6	6.3	87	$CO-H_2$	38	2633	458	POW1
103-17[f]	NA	NA	96	$H_2S-CO-H_2$	38	4050	438	ZAP2
Single Pass Operations[c]								
15-2[g]	(9)	(9.5)	NA	$CO-H_2$	27	4000	404	B3
26-7[g]	(7.8)	(6.4)	85	$CO-H_2$	28	3825	463	B3
26-11[g]	(8.3)	(5.3)	81	$CO-H_2$	29	3890	483	B3
32-3[h]	9.8	6.2	82	$CO-H_2$	32	3765	450	B3
34-4[h]	24	16	87	$CO-H_2$	70	4020	459	B3

[a]Yields in parenthesis are percentages of total SRL or SRC. Insufficient data is available to convert the number to a maf basis.

[b]Beulah and Indianhead are B3 and Zap2 Great Plains lignite samples; Big Brown is BB2 Gulf Coast lignite sample; and Powhattan is POW1 bituminous coal sample.

[c]Bottoms recycle utilized the product slurry containing ash, insolubles, and SRL as solvent for the subsequent pass in an open tubular reactor. Single pass utilized an anthracene oil and coal were passed through the reactor once (see DOE/GFETC/QTR-78/T4, NTIS).

[d]A heavy hydrogen donor (HAB1) was spiked each pass.

[e] Started up initially with a good H-donor solvent (HAB1).

[f]Feed gas ratio of CO to H_2 was 6:94. H_2S was nominally fed at 5 wt % of coal.

[g]CPU operation with a CSTR reactor and AO1-10% tetralin solvent.

[h]CPU operation with an open tubular reactor and AOD1 solvent (a distillate cut of AO1).

Table 2. Structural Features of Asphaltene Samples

RUN	PER	FRACT	WTPCT	VTRA[b]	Wt % C	H	N	O	S	MWVPO	OH	HTOC	HARUCAR	NMR[c] HAR	HAL	HOTH	Z[b]
15	2	0	100.00	.	83.75	6.09	0.81	8.15	1.21	500	1.853	0.872	0.852	36.3	48.3	12.4	0.7
15	2	1	5.33	.	81.73	6.30	0.91	9.85	1.21	2129	1.974	0.925	0.855	27.3	45.1	24.4	0.9
15	2	2	5.37	.	81.81	5.52	0.90	10.56	1.21	1510	1.986	0.809	0.671	22.3	40.3	33.8	0.1
15	2	3	8.52	.	81.61	5.86	0.77	10.54	1.22	1011	2.104	0.862	0.748	23.4	42.6	30.5	0.4
15	2	4	12.58	.	81.70	6.01	1.01	10.04	1.23	722	2.355	0.883	0.827	25.9	48.7	21.5	0.4
15	2	5	15.02	.	82.25	6.44	0.60	9.46	1.25	592	2.747	0.940	0.922	28.1	50.8	16.7	0.6
15	2	6	20.94	.	83.21	6.20	0.67	8.70	1.23	417	2.235	0.895	0.887	33.7	50.6	12.1	0.6
15	2	7	13.83	.	89.26	6.10	0.48	2.98	1.17	288	1.121	0.820	0.780	46.5	47.4	4.2	1.1
15	2	8	4.35	.	90.48	5.55	0.46	2.37	1.14	261	0.410	0.736	0.691	56.5	38.4	4.4	0.9
15	2	9	1.05	.	91.68	5.45	0.51	1.22	1.13	261	0.170	0.714	0.638	61.7	28.1	9.9	0.9
26	7	0	100.00	.	87.76	5.26	1.08	5.07	0.82	500	1.241	0.720	0.700	54.7	38.1	4.7	0.2
26	7	1	8.50	X	84.03	4.69	1.16	9.30	0.82	1663	1.231	0.669	0.640	50.1	30.6	16.6	-0.4
26	7	2	8.50	X	86.40	4.63	0.89	7.25	0.82	1104	1.241	0.644	0.608	50.8	34.2	12.3	-0.4
26	7	3	9.70	X	86.13	4.59	1.07	7.38	0.82	888	1.282	0.640	0.619	51.5	36.6	9.0	-0.5
26	7	4	9.70	.	86.25	4.95	0.87	7.10	0.83	595	1.412	0.689	0.664	50.5	37.5	9.2	-0.2
26	7	5	13.90	.	87.19	5.37	0.91	5.69	0.84	480	1.763	0.739	0.740	51.6	44.1	1.0	0.0
26	7	6	19.00	.	88.53	5.29	0.55	4.80	0.83	344	1.492	0.717	0.710	54.5	41.6	1.0	0.1
26	7	7	19.90	.	90.96	5.25	0.73	2.26	0.80	344	0.620	0.693	0.655	62.6	32.4	3.7	0.5
26	7	8	9.80	.	89.45	4.76	0.69	4.32	0.79	344	0.180	0.639	0.631	74.5	20.9	4.3	0.2
26	7	9	2.50	.	87.20	4.76	0.47	6.79	0.78	344	0.110	0.655	0.676	78.7	16.5	4.5	0.2
26	11	0	100.00	.	87.08	5.83	0.98	4.89	1.22	500	1.221	0.804	0.756	46.8	41.3	9.9	0.8
26	11	1	2.90	X	83.22	4.61	1.28	9.67	1.22	1556	1.282	0.665	0.592	37.4	36.2	23.6	-0.5
26	11	2	3.30	.	83.51	4.96	1.26	9.05	1.22	1205	1.282	0.713	0.628	37.9	35.0	24.5	-0.1
26	11	3	6.00	.	83.54	5.08	1.15	9.01	1.23	924	1.342	0.729	0.617	24.7	47.4	25.2	-0.0
26	11	4	11.00	.	84.61	5.58	1.02	7.57	1.23	690	1.442	0.791	0.694	37.1	37.6	22.8	0.4
26	11	5	15.00	.	84.74	5.61	0.88	7.51	1.25	517	1.833	0.794	0.734	38.0	42.3	16.4	0.2
26	11	6	30.00	.	86.63	5.82	0.64	5.68	1.24	353	1.602	0.806	0.804	46.4	48.4	2.5	0.6
26	11	7	14.80	.	90.70	5.65	0.17	2.30	1.18	267	0.380	0.748	0.704	56.0	39.5	3.9	1.0
26	11	8	22.30	X	91.89	5.32	0.33	1.29	1.16	261	9.000	0.695	0.662	69.9	27.4	2.6	-3.5
26	11	9	8.60	X	92.95	4.84	0.39	0.65	1.16	262	3.000	0.625	0.591	78.5	17.9	3.5	-1.1
32	3	0	97.00	.	84.35	5.95	1.22	7.93	0.55	390	2.571	0.846	0.808	40.9	39.7	15.2	0.2
32	3	1	3.10	.	83.16	5.43	2.06	8.82	0.54	1360	1.834	0.783	0.648	33.3	30.9	32.4	0.1
32	3	2	5.60	.	83.05	5.48	1.51	9.42	0.54	1540	2.043	0.791	0.697	35.3	34.2	26.8	0.0
32	3	3	6.90	.	84.04	5.77	1.48	8.16	0.55	1010	2.164	0.824	0.696	32.2	34.6	29.4	0.3
32	3	4	9.80	.	83.34	6.00	1.23	8.88	0.55	640	2.335	0.864	0.793	32.5	41.8	21.7	0.4
32	3	5	14.80	.	83.57	6.08	1.06	8.73	0.56	552	2.792	0.873	0.808	31.7	43.2	20.5	0.3
32	3	6	20.90	.	82.83	6.21	1.05	9.33	0.57	390	3.424	0.900	0.916	34.5	49.7	10.3	0.1
32	3	7	22.20	.	83.98	6.07	1.04	8.35	0.56	297	2.861	0.867	0.924	40.3	55.0	-0.0	0.2
32	3	8	12.10	.	88.94	5.72	0.91	3.91	0.52	242	0.970	0.771	0.767	56.8	41.6	-0.0	0.8
34	4	0	94.00	.	83.55	5.99	1.28	8.62	0.57	388	3.107	0.861	0.858	40.1	43.7	11.0	0.0
34	4	1	2.80	.	84.43	5.73	1.99	7.30	0.55	2330	2.221	0.815	0.614	27.8	29.6	38.7	0.2
34	4	2	5.30	.	84.58	5.68	2.06	7.13	0.55	1280	2.471	0.805	0.638	29.9	32.4	33.4	0.0
34	4	3	7.30	.	84.33	5.84	1.63	7.64	0.56	1050	2.663	0.831	0.691	31.1	34.2	30.2	0.1
34	4	4	10.80	.	84.31	6.00	1.56	7.56	0.56	765	2.969	0.854	0.736	30.5	38.5	26.1	0.1
34	4	5	16.40	.	83.93	6.18	1.38	7.93	0.57	550	3.502	0.884	0.815	31.5	42.9	20.0	0.0
34	4	6	21.70	X	83.02	6.16	1.36	8.87	0.59	374	4.377	0.890	0.909	33.7	50.9	8.3	-0.4
34	4	7	20.60	.	85.64	6.11	0.98	6.72	0.56	324	2.736	0.856	0.863	42.2	48.6	4.8	0.3
34	4	8	12.00	.	90.12	5.90	0.72	2.75	0.51	256	0.682	0.786	0.751	56.2	38.4	4.2	1.1
41	14	0	100.00	.	87.58	6.65	1.36	4.14	0.27	372	1.570	0.911	0.762	37.4	34.1	26.1	1.4
41	14	1	10.80	.	84.37	5.97	2.03	7.39	0.24	1250	1.493	0.849	0.661	29.1	31.7	36.7	0.8
41	14	2	5.40	.	85.51	7.03	1.52	5.69	0.24	740	1.532	0.986	0.691	23.2	27.8	46.9	1.8
41	14	3	7.30	.	86.09	6.98	1.43	5.28	0.21	645	1.593	0.973	0.713	23.8	32.2	41.7	1.7
41	14	4	11.40	.	85.84	6.95	1.22	5.78	0.22	470	1.842	0.971	0.784	27.5	36.0	33.9	1.6
41	14	5A	23.30	.	86.08	7.01	1.22	5.47	0.22	350	2.094	0.977	0.815	30.4	35.9	30.7	1.5
41	14	5B	28.50	.	88.37	6.30	1.25	3.87	0.21	280	0.985	0.856	0.740	42.7	35.6	20.2	1.4
41	14	5C	13.40	X	92.09	5.10	1.17	1.43	0.20	250	6.200	0.665	0.613	69.2	23.5	7.3	-2.4
44	12	0	100.00	.	88.52	5.57	0.87	4.71	0.32	378	0.962	0.755	0.694	54.2	31.0	13.1	0.6
45	15	0	100.00	.	88.68	6.39	1.17	3.48	0.27	384	1.599	0.865	0.759	43.8	35.4	18.3	1.1
46	16	0	100.00	.	90.10	5.93	1.09	2.55	0.32	333	1.136	0.790	0.704	54.5	29.2	14.4	0.9
46	16	1	9.20	.	86.34	5.51	1.53	6.39	0.23	876	1.247	0.765	0.607	40.5	24.0	33.3	0.4
46	16	2	22.90	.	87.16	6.22	1.09	5.33	0.19	431	1.464	0.857	0.727	38.9	33.6	25.1	1.0
46	16	3	25.90	.	88.69	6.27	1.17	3.66	0.21	290	1.124	0.848	0.771	47.1	37.3	13.8	1.3
46	16	4	25.80	.	91.65	5.74	0.68	1.73	0.20	250	0.399	0.751	0.697	62.5	29.8	7.0	1.1
46	16	5	16.20	X	93.37	5.06	0.64	0.73	0.20	260	5.300	0.650	0.621	81.1	15.1	3.7	-2.0
53	18	0	100.00	.	89.02	5.68	1.80	2.65	0.85	336	0.960	0.765	0.682	54.5	30.1	13.7	0.7
58	15	0	100.00	.	88.47	6.09	1.70	3.48	0.26	322	1.339	0.826	0.750	52.0	31.9	13.9	1.0
69	12	0	100.00	.	88.54	5.97	1.93	2.63	0.93	347	1.012	0.809	0.709	48.9	31.7	17.8	1.0

Table 2. Structural Features of Preasphaltene Samples

RUN	PER	FRACT	WTPCT	VTRA[b]	Wt % C	H	N	O	S	MWVPO	OH	HTOC	HARUCAR	NMR[c] HAR	HAL	HOTH	Z[b]
15	2	1	15.40	.	80.47	4.95	1.59	12.42	0.56	2716	1.801	0.739	0.690	35.1	35.7	25.6	-0.4
15	2	10	1.92	X	88.58	6.21	0.53	3.77	0.90	272	0.569	0.842	0.729	42.5	37.6	19.0	1.5
15	2	11	1.25	.	75.01	4.88	0.24	18.98	0.88	272	4.400	0.781	0.913	51.7	37.7	10.5	-1.7
15	2	12	0.60	.	84.88	5.21	0.35	8.68	0.88	272	5.000	0.737	0.742	55.9	36.1	8.0	-1.7
15	2	2	26.44	.	80.50	4.78	1.40	12.70	0.61	2497	1.878	0.713	0.668	35.4	35.2	25.5	-0.6
15	2	3	17.32	.	80.36	4.79	1.31	13.54	0.00	2055	1.973	0.716	0.702	34.4	40.6	20.9	-0.6
15	2	4	7.36	.	80.04	5.14	0.98	13.31	0.53	1228	2.377	0.771	0.778	31.6	47.3	16.5	-0.5
15	2	5	7.11	.	78.48	5.52	0.95	14.53	0.52	823	2.736	0.844	0.895	31.0	50.0	14.0	-0.3
15	2	6	7.70	.	78.15	5.79	0.97	14.55	0.53	619	2.949	0.890	0.966	30.4	52.4	12.1	-0.1
15	2	7	4.27	.	78.03	6.01	1.00	14.38	0.58	459	2.944	0.924	1.023	30.9	54.4	9.9	0.1
15	2	8	6.78	X	79.57	6.26	1.12	12.06	0.99	382	2.896	0.944	0.992	31.9	49.9	13.5	0.4
15	2	9	3.85	X	82.17	6.42	0.84	9.62	0.95	314	1.919	0.938	0.905	34.9	42.3	19.9	1.0
26	7	1	8.49	.	83.86	4.74	2.01	8.85	0.54	1874	1.381	0.678	0.658	53.4	29.3	14.3	-0.4
26	7	10	2.40	.	91.68	5.69	0.31	1.69	0.63	404	2.800	0.745	0.708	65.6	30.8	3.6	-0.1
26	7	2	23.36	.	85.31	4.66	1.73	7.50	0.80	1496	1.479	0.656	0.616	50.7	31.6	14.5	-0.5
26	7	3	19.60	.	83.91	4.74	1.47	9.31	0.58	1314	1.694	0.678	0.677	55.5	29.5	11.5	-0.6
26	7	4	13.52	.	82.80	5.02	1.36	10.08	0.73	640	2.261	0.728	0.761	46.4	44.8	4.3	-0.5
26	7	5	8.40	.	82.69	5.46	1.29	10.01	0.55	488	3.037	0.792	0.831	38.9	51.9	3.6	-0.5
26	7	6	7.84	.	81.63	5.74	1.20	10.76	0.67	404	3.338	0.844	0.909	41.2	49.9	3.1	-0.4
26	7	7	6.08	.	83.98	6.03	1.09	8.18	0.72	404	3.227	0.862	0.886	41.1	48.4	5.2	-0.0
26	7	8	4.96	X	88.06	6.16	0.49	4.62	0.66	404	1.255	0.839	0.810	46.4	44.4	7.2	1.1
26	7	9	4.96	X	90.61	6.05	0.32	2.38	0.64	404	0.205	0.801	0.746	55.3	37.4	7.0	1.5
26	11	1	21.68	.	85.79	4.61	1.49	7.63	0.48	1039	1.021	0.645	0.623	56.8	28.9	12.1	-0.4
26	11	2	31.24	.	86.03	4.73	1.34	7.41	0.50	829	1.426	0.659	0.645	54.2	33.9	8.9	-0.4
26	11	3	22.22	.	85.67	4.79	1.35	7.70	0.49	621	1.501	0.671	0.671	54.7	35.8	6.3	-0.4
26	11	4	9.17	.	84.88	4.82	1.32	8.29	0.69	480	1.882	0.682	0.695	53.0	38.6	4.5	-0.6
26	11	5	3.03	X	84.81	5.54	0.93	8.06	0.67	480	0.985	0.784	0.799	55.5	37.0	5.7	0.6
26	11	6	1.86	X	90.56	5.56	0.36	2.87	0.65	480	0.212	0.736	0.696	62.2	31.5	5.9	1.0
26	11	7	0.78	.	91.23	5.28	0.23	2.61	0.64	480	3.900	0.695	0.666	71.1	24.0	4.8	-1.1
26	11	8	0.15	.	91.32	5.27	0.61	2.15	0.64	480	3.200	0.693	0.645	74.0	16.2	9.7	-0.8
32	3	0	97.00	.	83.22	5.06	2.16	8.99	0.57	588	3.115	0.730	0.721	40.8	43.2	9.9	-0.9
32	3	1	16.20	.	83.78	4.53	2.30	8.85	0.54	1320	1.912	0.649	0.564	39.8	29.7	26.3	-0.9
32	3	2	19.90	.	83.38	4.70	2.40	8.97	0.55	1800	2.376	0.677	0.647	42.2	38.8	14.0	-0.9
32	3	3	13.30	.	82.37	4.95	2.15	9.97	0.56	837	2.935	0.721	0.696	41.8	35.8	16.5	-0.9
32	3	4	12.40	.	83.01	5.07	2.39	8.93	0.59	648	4.374	0.732	0.747	42.7	43.0	5.7	-1.5
32	3	5	13.00	.	81.25	5.36	1.94	10.86	0.58	570	3.714	0.792	0.839	45.3	42.0	5.7	-0.9
32	3	6	11.30	.	80.25	5.56	1.88	11.72	0.59	397	4.179	0.831	0.888	40.2	45.2	7.1	-0.9
32	3	7	8.80	.	76.52	6.04	1.95	14.91	0.59	290	4.053	0.946	1.046	33.6	47.1	12.6	-0.4
32	3	8	2.70	X	83.95	6.25	2.53	6.72	0.55	241	2.291	0.893	0.804	34.6	40.4	21.4	0.7
34	4	0	97.00	.	83.49	5.07	2.15	8.73	0.56	612	2.824	0.729	0.715	41.2	43.0	10.2	-0.8
34	4	1	13.60	.	83.58	4.55	2.73	8.61	0.53	2020	1.616	0.653	0.550	37.4	30.5	28.5	-0.7
34	4	2	24.30	.	83.58	4.72	2.44	8.72	0.54	1780	1.925	0.677	0.600	39.5	33.1	23.3	-0.7
34	4	3	13.90	.	82.98	5.03	2.57	8.88	0.55	940	2.525	0.727	0.694	39.8	40.9	14.2	-0.7
34	4	4	12.20	.	82.50	5.18	2.26	9.50	0.56	690	2.957	0.753	0.738	38.7	43.4	12.2	-0.7
34	4	5	12.60	.	81.24	5.30	1.96	10.92	0.57	470	3.187	0.783	0.804	39.6	44.7	9.7	-0.7
34	4	6	9.80	.	80.53	5.40	2.00	11.49	0.57	390	3.545	0.805	0.848	37.8	48.2	7.5	-0.8
41	14	0	100.00	.	85.27	5.17	1.98	7.35	0.24	671	1.790	0.727	0.631	43.5	28.3	24.7	-0.2
41	14	1	21.40	.	86.72	4.47	1.56	7.03	0.21	2850	1.321	0.619	0.530	47.8	24.0	25.2	-0.6
41	14	2	16.60	.	85.00	4.73	2.01	8.05	0.21	1420	1.603	0.667	0.590	45.2	28.0	23.5	-0.5
41	14	3	26.10	.	84.48	5.02	1.91	8.44	0.15	740	2.010	0.713	0.661	44.5	33.4	18.1	-0.4
41	14	4	24.10	.	83.96	5.51	1.81	8.50	0.22	430	2.492	0.788	0.744	41.5	37.3	16.6	-0.2
41	14	5	11.80	X	86.90	6.02	1.65	5.23	0.21	290	1.102	0.831	0.679	42.2	26.6	29.3	1.0
44	12	0	100.00	.	87.76	4.90	1.44	5.69	0.21	600	1.540	0.670	0.621	58.8	23.5	14.6	-0.3
45	15	0	100.00	.	85.58	5.28	1.57	7.42	0.15	676	1.783	0.740	0.649	43.3	29.9	23.4	-0.1
46	16	0	100.00	.	88.48	4.85	1.44	4.80	0.44	608	1.604	0.657	0.609	59.0	25.5	12.2	-0.4
46	16	1	15.50	.	87.64	4.12	2.03	6.07	0.14	2650	0.808	0.564	0.531	69.5	12.0	16.6	-0.7
46	16	2	14.40	.	87.16	4.28	1.90	6.48	0.18	1420	1.232	0.589	0.551	61.7	19.6	15.9	-0.8
46	16	3	23.10	.	86.52	4.46	1.81	6.99	0.21	806	1.426	0.619	0.584	57.7	24.6	14.6	-0.7
46	16	4	25.60	.	86.64	4.93	1.58	6.69	0.16	390	1.777	0.683	0.650	54.7	29.7	12.0	-0.4
46	16	5	21.30	X	87.29	5.60	1.41	5.49	0.21	290	0.861	0.770	0.695	54.2	25.9	18.4	0.7
53	18	0	100.00	.	85.80	4.55	2.28	6.51	0.87	701	1.433	0.636	0.568	53.9	23.3	19.6	-0.6
58	15	0	100.00	.	86.68	5.05	2.50	5.62	0.15	620	1.804	0.699	0.631	53.8	25.0	17.6	-0.3
69	12	0	100.00	.	86.56	4.88	2.47	5.16	0.93	702	1.177	0.676	0.584	52.1	23.9	21.6	-0.2

Table 2. Structural Features of 103[a]

					Wt %									NMR[c]				
RUN	PER	FRACT	WTPCT	VTRA[b]	C	H	N	O	S	MWVPO	OH	HTOC	HARUCAR	HAR	HAL	HOTH	Z[b]
103	17	0	100.00	.	87.77	5.62	1.70	4.67	0.24	560	2.120	0.768	d	-	-	-	0.1
103	17	1	16.60	.	87.51	4.57	1.90	5.67	0.34	1600	0.690	0.627	-	-	-	-	-0.2
103	17	2	11.40	.	84.67	5.36	2.46	6.77	0.73	930	1.470	0.760	-	-	-	-	0.2
103	17	3	14.30	.	86.10	5.76	2.12	5.65	0.37	510	1.920	0.803	-	-	-	-	0.4
103	17	4	19.80	.	85.51	6.06	1.82	6.04	0.57	330	2.460	0.851	-	-	-	-	0.4
103	17	5	21.70	.	85.59	6.39	1.47	6.26	0.29	140	2.050	0.896	-	-	-	-	0.9
103	17	6	14.10	.	87.07	6.11	1.21	5.17	0.45	140	0.940	0.842	-	-	-	-	1.2

a. 103 is a total SRL containing both asphaltenes and preasphaltenes.
b. X in VTRA indicates Z = H% - 0.486(OH) - 4.67 mismatch. If Z = negative sample is a preasphaltene. If Z = positive sample is an asphaltene.
c. $H_{ar} + H_{al} + H_{OH} = 100$, sum of mole fractionof aromatic, aliphatic and phenolic protons equals 100. To obtain H_{OH} subtract $H_{ar} + H_{al}$ from 100. H_o equals mole percent of protons on aliphatic carbons more than one carbon unit from an aromatic ring, alpha + other protons equals total aliphatic protons.
d. Data not measured.

Table 3. Correlation Coefficients (r) Between Various Asphaltene and Preasphaltene Parameters

Asphaltenes	r value			
Parameter	H[a]	H/M[b]	H/C[c]	H_{aru}/C_{ar}[d]
H	1.0	0.996	0.943	0.56
H/M	---	1.0	0.970	0.60
H/C	---	---	1.0	0.64
H_{aru}/C_{ar}	---	---	---	1.00
OH	-0.14	-0.13	-0.100	0.03

Preasphaltenes				
Parameter	H	H/M	H/C	H_{aru}/C_{ar}
H	1.0	0.998	0.97	0.91
H/M	---	1.0	0.98	0.93
H/C	---	---	1.0	0.96
H_{aru}/C_{ar}	---	---	---	1.0
OH	0.78	0.793	0.82	0.83

a. Mole fraction of hydrogen (wt %).
b. Mole ratio of H/(C+N+O+S).
c. Molar H/C ratio.
d. Mole ratio of edge aromatic to aromatic carbon.

Table 4. Molecular Weight Values for Runs 46 and 32

Sample	Molecular Weight[a] Asphaltene	Preasphaltene
46-1	875	2650
46-2	430	1420
46-3	290	810
46-4	250	390
46-5	260	290
32-1	1360	1320
32-2	1540	1800
32-3	1010	840
32-4	640	650
32-5	550	570
32-6	390	400
32-7	300	---

[a]determined by VPO, solvent pyridine

Table 5. Comparison of Oxygen Functionality for Various Asphaltene (A) and Preasphaltene (PA) Samples

Sample	Recycle[a]	Oxygen Content mmoles/g Total O_2	Phenol	% O_2 as phenol
41 PA	yes	4.39	1.79	41
41 A	yes	2.48	1.57	63
45 PA	yes	4.42	1.78	40
45 A	yes	2.09	1.60	77
53 PA	yes	3.92	1.43	37
53 A	yes	1.61	0.96	60
69 PA	yes	3.13	1.12	36
69 A	yes	1.60	1.01	63
103 Total[b]	yes	2.91	2.12	73
32 PA	no	5.61	3.12	55
32 A	no	5.51	2.57	52
15 PA	no	7.89	2.11	17
15 A	no	5.09	1.85	36
26 PA	no	5.16	1.89	37
26 A	no	3.16	1.24	40

[a]No indicates petroleum derived solvent passed once through. Yes indicates bottom recycle solvent used.

[b]In this case asphaltene and preasphaltene sample not separated. H_2S run.

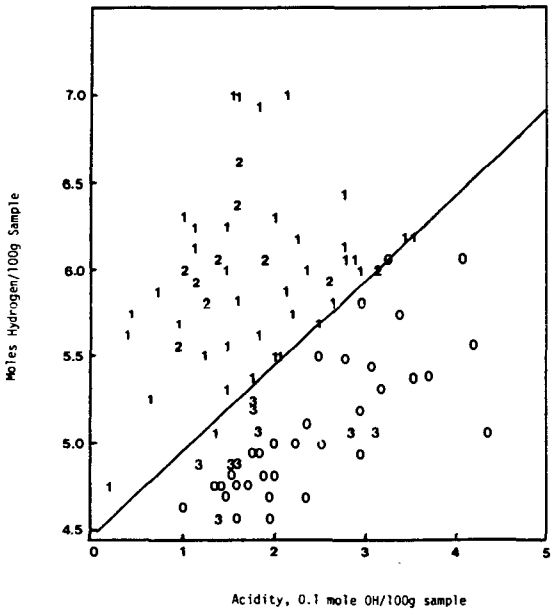

Figure 1 The hydrogen and acid content of asphaltene (1) and preasphaltene (0) fractions. Total preasphaltene (3) and asphaltene (2). Samples (unfractionated) are also plotted.

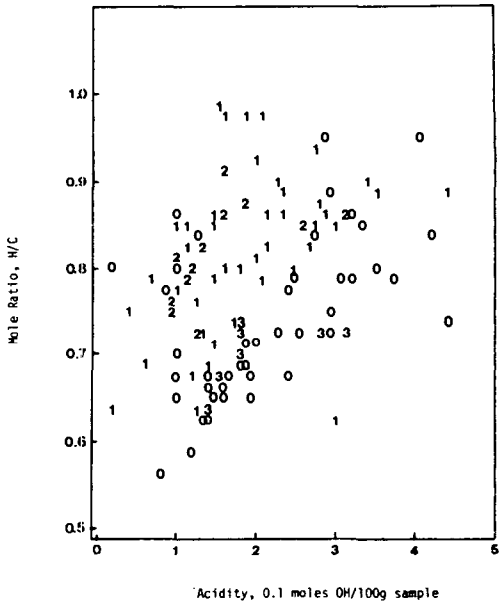

Figure 2 The relationship of H/C mole ratio to acidity of asphaltene (1), and preasphaltene (0) fractions. Total preasphaltenes (3) and total asphaltenes (2) are also plotted (unfractionated).

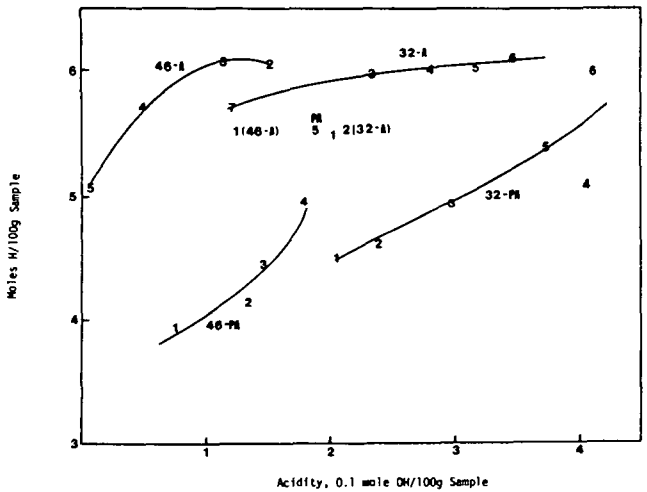

Figure 4 Hydrogen and phenolic hydroxyl dependence of Runs 32 and 46. A=Asphaltene, PA=Preasphaltene; Molecular wt decreases with fraction number 1-7.

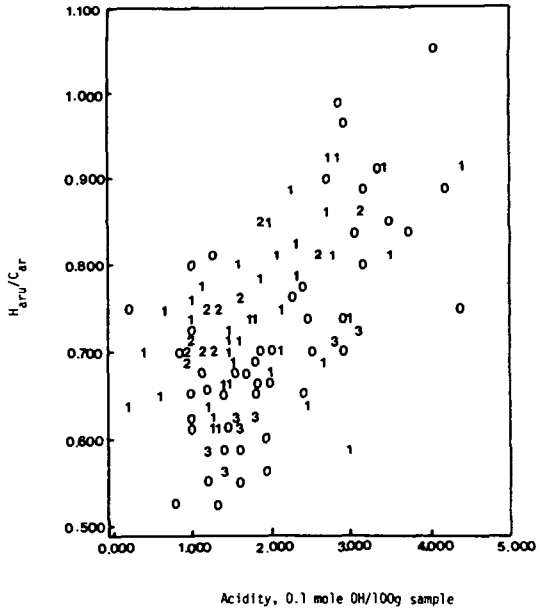

Figure 3 The degree of condensation and acidity of asphaltene (1) and preasphaltene (0) fractions. Total preasphaltene (3) and asphaltene (2) samples (unfractionated) are also plotted.